Non-Linear Effects in Plasmas

Notes to the course on Plasma Instabilities
given in the frame of the Doctoral School of Physics, EPFL.

Stephan Brunner
stephan.brunner@epfl.ch

Swiss Plasma Center (SPC),
Ecole Polytechnique Fédérale de Lausanne (EPFL),
CH-1015 Lausanne, Switzerland

Last modified: December 10, 2019

Contents

Chapter 1

Non-Linear Effects in Plasmas

1.1 Introduction

For many plasmas of interest, the Vlasov-Maxwell system of equations can be considered as the "fundamental" kinetic description:

- The Vlasov equation describes how the evolution of the phase space distribution $f_\alpha(\vec{x}, \vec{v}, t)$ for each plasma species α (= electrons "e", ions "i") is subject to macroscopic electric and magnetic fields $(\vec{E}, \vec{B})$:

$$\frac{\partial f_\alpha}{\partial t} + \vec{v} \cdot \frac{\partial f_\alpha}{\partial \vec{x}} + \frac{q_\alpha}{m_\alpha} \left(\vec{E} + \vec{v} \times \vec{B} \right) \cdot \frac{\partial f_\alpha}{\partial \vec{v}} = 0. \tag{1.1}$$

  This equation is justified in the limit of weakly coupled plasmas, characterized by a small value $\epsilon_p \ll 1$ of the plasma parameter $\epsilon_p = 1/(N\lambda_D^3) \sim N^{1/2}T^{-3/2}$ (N is the density, T the temperature, and λ_D the Debye length). One recalls, that the parameter ϵ_p is a measure of the relative fluctuation level of interaction energy due to particle discreteness compared to the kinetic energy. The weakly coupled approximation is justified for handling most plasmas of interest in magnetic fusion, *i.e.* plasmas with low density and high temperature.

- In turn, Maxwell's equations describe the evolution of the fields $[\vec{E}(\vec{x}, t), \vec{B}(\vec{x}, t)]$:

$$\nabla \times \vec{E} = -\frac{\partial \vec{B}}{\partial t}, \qquad \nabla \times \vec{B} = \mu_0 \vec{j} + \frac{1}{c^2}\frac{\partial \vec{E}}{\partial t}, \tag{1.2}$$

$$\nabla \cdot \vec{B} = 0, \qquad \nabla \cdot \vec{E} = \frac{\rho}{\epsilon_0}, \tag{1.3}$$

  where the charge density ρ and current density $\vec{j}$ are generated by the plasma itself:

$$\rho^{\text{int}} = \sum_\alpha q_\alpha \int d\vec{v}\, f_\alpha, \qquad \vec{j}^{\text{int}} = \sum_\alpha q_\alpha \int d\vec{v}\, \vec{v}\, f_\alpha, \tag{1.4}$$

  as well as by possible external sources $(\rho^{\text{ext}}, \vec{j}^{\text{ext}})$, so that in general:

$$\rho = \rho^{\text{int}} + \rho^{\text{ext}}, \qquad \vec{j} = \vec{j}^{\text{int}} + \vec{j}^{\text{ext}}. \tag{1.5}$$

The system of equations (1.1)-(1.5) clearly show how the plasma is both *subject to*, and *the source of*, electromagnetic fields. The distributions f_α and the fields $(\vec{E}, \vec{B})$ must therefore be solved for self-consistently.

Note furthermore, that in terms of the unknown quantities f_α and $(\vec{E}, \vec{B})$, equations (1.1)-(1.5) form a non-linear system of integro-differential equations. Indeed, the last term in Vlasov's equations (1.1) represents a quadratic non-linearity. This is in fact the only non-linear term in this system, as Maxwell's equation are themselves fully linear [including the evaluation of the sources $(\rho^{\text{int}}, \vec{j}^{\text{int}})$ in terms of f_α].

Although collisional effects will not be discussed in any detail in this chapter, let us nonetheless briefly comment here on the additional non-linearity found in the more general Fokker-Planck equation. Indeed, in cases for which the fluctuations due to binary scattering effects can not be fully neglected, the Vlasov equation is replaced by the more general Fokker-Planck equation:

$$\frac{\partial f_\alpha}{\partial t} + \vec{v} \cdot \frac{\partial f_\alpha}{\partial \vec{x}} + \frac{q_\alpha}{m_\alpha} \left(\vec{E} + \vec{v} \times \vec{B} \right) \cdot \frac{\partial f_\alpha}{\partial \vec{v}} = \sum_\beta C[f_\beta, f_\alpha],$$

where the collision operator $C[f_\beta, f_\alpha]$ represents the scattering of species α off of species β. This collision operator can in many cases be modeled by the Landau-type operator:

$$C[f_\beta, f_\alpha] = \Gamma_{\alpha,\beta} \frac{\partial}{\partial \vec{v}} \cdot \int d\vec{v}\,' \, \mathbf{U}(\vec{v} - \vec{v}\,') \cdot \left(\frac{1}{m_\beta} \frac{\partial}{\partial \vec{v}\,'} - \frac{1}{m_\alpha} \frac{\partial}{\partial \vec{v}} \right) f_\beta(\vec{v}\,') f_\alpha(\vec{v}), \tag{1.6}$$

where $\Gamma_{\alpha,\beta} = q_\alpha^2 q_\beta^2 \ln \Lambda / (8\pi\epsilon_0^2 m_\alpha)$, $\ln \Lambda$ is the Coulomb logarithm, and one has defined the tensor $\mathbf{U}(\vec{u}) = (u^2 \mathbf{1} - \vec{u} : \vec{u})/u^3$. The collision operator scales as $C \sim \nu_c f$, where the collision frequency ν_c is of the order $\nu_c/\omega_p \sim \mathcal{O}(\epsilon_p)$, ω_p being the plasma frequency. The collision operator (1.6) obviously provides an additional non-linearity to the Fokker-Planck equation. The origin of this non-linearity is similar to the one in the Vlasov part of the equation, i.e. the effect of self-consistent electromagnetic fields on the distribution. The non-linearity in C however results from the Coulomb forces relative to random binary interactions, while the non-linearity in the Vlasov part results from the macroscopic electro-magnetic fields from collective phenomena.

For understanding certain basic mechanisms, one can justify linearizing the Vlasov-Maxwell system of equations. It is assumed here that the reader is familiar with this linear approximation, in particular as a first approach to studying the dispersion and dissipation of small amplitude waves. However, plasmas are fundamentally non-linear in nature, and the non-linearities pointed out above are thus essential for describing a whole set of important plasma phenomena.

Non-linear plasma theory is a vast topic, and this chapter only provides an introduction to the subject through a couple of specific examples. The first part of this chapter considers the non-linear evolution of a single, finite amplitude Langmuir wave, and in particular points out the break down of linear Landau damping. To model the non-linear evolution of resonant wave-particle interaction naturally requires the framework of a kinetic description. The second part of this chapter addresses the issue of non-linear wave-wave interaction, and in particular the mechanism of parametric instabilities. These wave-wave interactions do not involve resonant particles in their basic form, and thus can be derived from fluid equations.

The examples of non-linear phenomena considered in this chapter are all cases of weak non-linearity, for which the wave energy remains small compared to the total plasma energy. Under these conditions, the dispersion of the considered waves remains near the dispersion predicted by linear theory (some non-linear corrections may nonetheless occur, see the section on non-linear frequency shift), so that non-linear effects mainly affect the evolution of the amplitudes of the waves, by either altering damping in the case of non-linearly interacting resonant particles, or by providing coupling between waves in the case of wave-wave interactions.

General Reference: Sagdeev and Galeev Ref. [1].

1.2 Non-Linear Evolution of an Electron Plasma Wave

1.2.1 Motivation/Illustration

In the following, the terms "Langmuir wave" and "electron plasma wave" (EPW) are used interchangeably to describe the high frequency (near ω_p), electrostatic plasma oscillations.

Figure 1.1 presents results from non-linear Vlasov-Poisson simulations of Langmuir waves using the SAPRISTI code[1]. In this case, the code simply solves the 1-Dim Vlasov-Poisson system of equations, where only the electron distribution $f_e(x, v, t)$ is evolved:

$$\frac{\partial f}{\partial t} + v\frac{\partial f}{\partial x} - \frac{e}{m}E\frac{\partial f}{\partial v} = 0, \qquad \frac{\partial E}{\partial x} = \frac{1}{\epsilon_0}\left(-e\int dv f + q_i N_{i,0}\right). \tag{1.7}$$

For studying Langmuir waves, it is a good approximation to assume that the ions form a fixed, homogeneous, neutralizing background, with density $N_{i,0}$. Here, and in the following, one drops the subscript "e" for electronic quantities, unless required for clarity.

For practical reasons, it is simpler to initiate a standing wave than a propagating wave. This is done by choosing the initial electron distribution as a Maxwellian with a sinusoidal density perturbation δN:

$$f_0(x, v) = \left[1 + \frac{\delta N}{N}\cos(k_0 x)\right] f_M(v), \qquad f_M(v) = \frac{N}{(2\pi)^{1/2} v_{\text{th}}}\exp(-\frac{v^2}{2v_{\text{th}}^2}).$$

Figures 1.1 a) and b) present the evolution of the potential energy, the variation of kinetic energy, and the total energy for initial conditions with perturbation levels $\delta N/N = 0.01$ and 0.1 respectively. For these illustrations, the wavelength is chosen such that $k_0\lambda_D = 0.3$, where $\lambda_D = v_{\text{th}}/\omega_p$ is the Debye length, and $\omega_p^2 = Ne^2/m\epsilon_0$ the squared plasma frequency. By numerically solving the linear dispersion relation for Langmuir waves, one obtains for $k_0\lambda_D = 0.3$: Frequency $\omega_0/\omega_p = 1.1598$, and linear Landau damping rate $\gamma_L/\omega_p = 1.2620 \cdot 10^{-2}$.

Note, that throughout the simulation the total energy E_{tot} (= Kinetic energy Kin of electrons + Electrostatic potential energy Pot):

$$E_{\text{tot}} = \text{Kin} + \text{Pot} = \frac{m}{2}\int_0^{\lambda_0} dx \int dv\, v^2 f \;+\; \frac{\epsilon_0}{2}\int_0^{\lambda_0} dx\, E^2,$$

remains essentially constant. This is naturally expected as E_{tot} is conserved by the system of Eqs. (1.7) (check it!).

As shown in Fig. 1.1.a, the very first stage of the wave's evolution in the non-linear

[1] The acronym stands for (S)emi-Lagrangian (A)dvection code for (P)a(R)ametric (I)n(ST)ab(I)lity studies. You are welcome to use this Fortran 90 code to familiarize with the different physical mechanisms addressed in this chapter. It is available on the SVN web server of the CRPP.

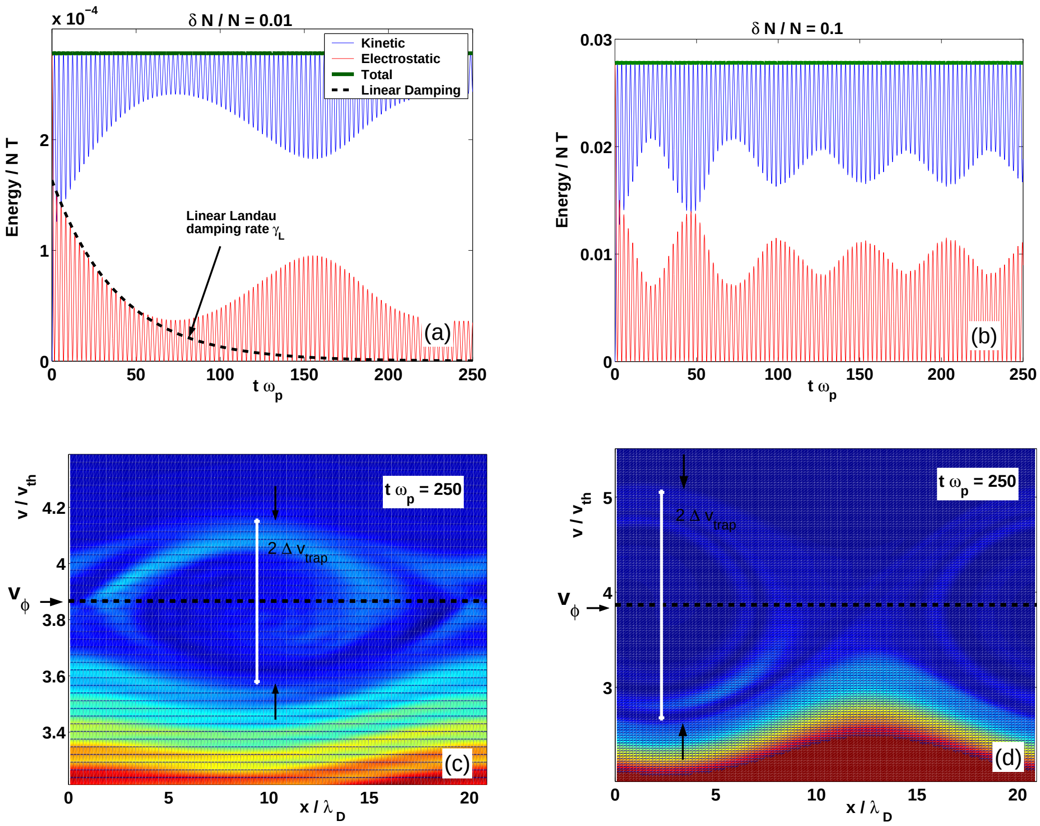

Figure 1.1: Results from Vlasov-Poisson simulations. Non-linear evolution of a standing Langmuir wave. Potential energy, and variation of kinetic energy for initial density perturbation (a) $\delta N/N = 0.01$ and (b) $\delta N/N = 0.1$ respectively. Distribution in phase space at $t\omega_p = 250$ for (c) $\delta N/N = 0.01$ and (d) $\delta N/N = 0.1$ respectively.

simulation is clearly exponential, and in agreement with the estimate γ_L for the Landau damping from the linear theory. At later times however, the wave's amplitude starts to *oscillate*. This oscillation ultimately dies out, and the wave amplitude *settles at a finite value*. The asymptotic state of the system is thus an undamped mode. These are obviously features not predicted by the linear theory of Landau damping. Figures 1.1 c) and d) show the electron distribution at time $t = 250\,\omega_p^{-1}$ in phase space (x, v) near the phase velocity $v_\phi = \omega_0/k_0$ for both cases $\delta N/N = 0.01$ and 0.1 respectively. These phase-space plots clearly illustrate trapping for particles with velocity v in an interval of width $2\Delta v_{\text{trap}}$ around v_ϕ.

The purpose of the following sections is to study the non-linear effects illustrated by these simulation results. For experimental confirmation of these effects, see the work by Danielson [3] and the references therein.

In the following sections, the evolution of a traveling Langmuir wave will be considered, while the simulation results just presented here involve standing waves. So, will the following discussion apply to these results? Yes, but why? A standing wave can naturally be considered as the superposition of a forward traveling wave with phase velocity v_ϕ, and a backward traveling wave with phase velocity $-v_\phi$. However, as one considers here non-linear phenomena, one must be careful before invoking a superposition principal. As will be discussed in detail, the non-linearities affecting each of these waves involve the corresponding resonant particles, i.e. particles with velocities within an interval of order Δv_{trap} from the corresponding phase velocity. As in general $\Delta v_{\text{trap}}/v_\phi \ll 1$, the resonant particles relative to the forward and backward traveling waves thus usually form two distinct groups with velocities in the vicinity of v_ϕ and $-v_\phi$ respectively. For this reason the two traveling components forming a standing Langmuir wave can be assumed non-interacting.

1.2.2 Re-Deriving Linear Landau Damping Invoking Energy Conservation

One considers an initially Maxwellian, homogeneous plasma. The study is limited here to the evolution of an electron plasma wave, so that ions may be assumed fixed, providing a neutralizing background for the mobile electrons.

One considers a slab-like system, so that the electron distribution $f(x, v, t)$ verifies the 1-Dim Vlasov equation:

$$\frac{\partial f}{\partial t} + v\frac{\partial f}{\partial x} - \frac{e}{m}E\,\frac{\partial f}{\partial v} = 0.$$

One furthermore assumes the electrostatic wave to be essentially monochromatic of the form:

$$E(x, t) = E_0(t)\sin(k_0 x - \omega_0 t),$$

where the amplitude $E_0(t)$ evolves at a slow time scale compared to the frequency ω_0. i.e. $|(dE_0/dt)/E_0| \ll \omega_0$.

One is interested here in the rate of change of the kinetic energy Kin of the electrons in the field $E(x,t)$. The spatially averaged kinetic energy is defined by

$$\mathrm{Kin} = \frac{m}{2}\int dv\, v^2 \langle f\rangle_x,$$

where the brackets $\langle\rangle_x$ stand for the spatial average:

$$\langle\rangle_x = \frac{1}{\lambda_0}\int_0^{\lambda_0} dx,$$

$\lambda_0 = 2\pi/k_0$ being one wavelength of the electrostatic field, which can be considered here as the length of the periodic system.

The rate of change is then given by

$$\frac{d\,\mathrm{Kin}}{dt} = \frac{m}{2}\int dv\, v^2 \langle\frac{\partial f}{\partial t}\rangle_x. \tag{1.8}$$

One starts by considering a perturbative approach, so that the distribution is expanded as

$$f = f_0(v) + f_1(x,v,t) + f_2(x,v,t) + \ldots,$$

where $f_n \sim \mathcal{O}(E^n)$, and f_0 is the initial unperturbed state. Expanding the Vlasov Eq. for the first two perturbation orders leads to

$$\frac{\partial f_1}{\partial t} + v\frac{\partial f_1}{\partial x} - \frac{e}{m}E\,\frac{\partial f_0}{\partial v} = 0, \tag{1.9}$$

$$\frac{\partial f_2}{\partial t} + v\frac{\partial f_2}{\partial x} - \frac{e}{m}E\,\frac{\partial f_1}{\partial v} = 0. \tag{1.10}$$

Obviously $\langle\partial f_0/\partial t\rangle_x = 0$ as $f_0 \neq f_0(t)$, and also $\langle\partial f_1/\partial t\rangle_x = 0$ as $f_1 \sim E \sim \cos(k_0 x - \omega_0 t)$ from Eq. (1.9). Thus, to lowest order in the perturbation, equation (1.8) is evaluated by

$$\begin{aligned}\frac{d\,\mathrm{Kin}}{dt} &= \frac{m}{2}\int dv\, v^2\langle\frac{\partial f_2}{\partial t}\rangle_x = \frac{e}{2}\int dv\, v^2\langle E\,\frac{\partial f_1}{\partial v}\rangle_x \\ &= -e\int dv\, v\langle E\, f_1\rangle_x,\end{aligned} \tag{1.11}$$

having made use of Eq. (1.10), $\langle\partial f_2/\partial x\rangle_x = 0$, and performed an integration by parts in the last step. Note that the last equality in Eq. (1.11) simply corresponds to $d\mathrm{Kin}/dt = \langle\vec{j}\cdot\vec{E}\rangle_x$, where $\vec{j}$ is the electronic charge current.

One now addresses the problem of deriving $\langle E\, f_1\rangle_x$. The linear perturbation f_1 can be obtained from Eq.(1.9) by integrating along the unperturbed trajectories. Indeed, Eq. (1.9) can be written as

$$\left.\frac{df_1}{dt}\right|_{\mathrm{u.t.}} = \frac{e}{m}E\,\frac{\partial f_0}{\partial v}, \tag{1.12}$$

where $d/dt|_{\text{u.t.}}$ stands for the total time derivative along the unperturbed trajectories (for more details on solving Vlasov-type equations by integrating along trajectories, see Appendix B). For the here considered homogeneous, unmagnetized plasma, the unperturbed trajectories are simply given by (free streaming):

$$\begin{aligned} \frac{dx'}{dt'} &= v', & \frac{dv'}{dt'} = 0, \\ \text{with initial conditions} \quad x'(t) &= x, & v'(t) = v, \end{aligned}$$

whose solution is $x' = x + v(t' - t)$ and $v' = v$. Equation(1.12) can thus be solved by integrating along these characteristics:

$$\begin{aligned} f_1(x, v, t) - f_1(x - vt, v, 0) &= \int_0^t dt' \left. \frac{df_1(x', v', t')}{dt'} \right|_{\text{u.t.}} = \frac{e}{m} \int_0^t dt'\, E(x', t')\, \frac{\partial f_0(v')}{\partial v} \\ &= \frac{e}{m} \frac{\partial f_0}{\partial v} \int_0^t dt'\, E_0(t') \sin\left[k_0 x + k_0 v(t' - t) - \omega_0 t'\right]. \end{aligned} \tag{1.13}$$

As $E(x, t)$ is assumed a self-consistent field, the initial perturbation $f_1(x, v, 0)$ must be such that Poisson's equation is verified at $t = 0$:

$$\frac{\partial E(x, 0)}{\partial x} = k_0 E_0(0) \cos(k_0 x) = \frac{-e}{\epsilon_0} \int dv\, f_1(x, v, 0).$$

This equation is verified for

$$f_1(x, v, 0) = f_{1,0}(v) \cos(k_0 x), \tag{1.14}$$

with $f_{1,0}(v)$ such that

$$\int dv\, f_{1,0}(v) = -\frac{\epsilon_0\, k_0}{e} E_0(0).$$

Combining (1.13) and (1.14), one thus obtains for the linear perturbation:

$$f_1(x, v, t) = f_{10}(v) \cos[k_0(x - vt)] + \frac{e}{m} \frac{\partial f_0}{\partial v} \int_0^t dt'\, E_0(t') \sin\left[k_0 x + k_0 v(t' - t) - \omega_0 t'\right]. \tag{1.15}$$

The first term on the right hand side of Eq.(1.15) is a free streaming term, and therefore is a transient, as will appear clearly further on. The second term is related to the actual coherent wave.

Equation (1.15) can now be used for computing $\langle E\, f_1 \rangle_x$:

$$\begin{aligned} \langle E\, f_1 \rangle_x &= E_0(t) f_{10}(v) \left\langle \sin(k_0 x - \omega_0 t) \cos[k_0(x - vt)] \right\rangle_x \\ &\quad + \frac{e}{m} \frac{\partial f_0}{\partial v} E_0(t) \int_0^t dt'\, E_0(t') \left\langle \sin(k_0 x - \omega_0 t) \sin\left[k_0 x + k_0 v(t' - t) - \omega_0 t'\right] \right\rangle_x \\ &= \frac{1}{2} E_0(t) f_{10}(v) \sin[(k_0 v - \omega_0) t] \\ &\quad + \frac{1}{2} \frac{e}{m} \frac{\partial f_0}{\partial v} E_0(t) \int_0^t dt'\, E_0(t') \cos\left[(k_0 v - \omega_0)(t' - t)\right], \end{aligned} \tag{1.16}$$

having applied the relation $\langle \sin(k_0 x+\alpha)\sin(k_0 x+\beta)\rangle_x = (1/2)\cos(\alpha-\beta)$.

The time integral in the second term of this last relation can be carried out after Taylor expanding the electrostatic field amplitude $E_0(t') = E_0(t)+(dE_0(t)/dt)(t'-t)+\ldots$, which is justified by invoking the assumption $|(dE_0/dt)/E_0| \ll \omega_0$, so that

$$\begin{aligned}
&\int_0^t dt'\, E_0(t')\cos\left[(k_0 v-\omega_0)(t'-t)\right] \\
&= E_0(t)\int_0^t dt'\, \cos\left[(k_0 v-\omega_0)(t'-t)\right] + \frac{dE_0(t)}{dt}\int_0^t dt'\,(t'-t)\cos\left[(k_0 v-\omega_0)(t'-t)\right] \\
&= E_0(t)\frac{\sin[(k_0 v-\omega_0)t]}{k_0 v-\omega_0} + \frac{dE_0(t)}{dt}\frac{\partial}{\partial\omega_0}\frac{1-\cos[(k_0 v-\omega_0)t]}{k_0 v-\omega_0},
\end{aligned} \tag{1.17}$$

having used $\int d\tau\,\tau\cos[(k_0 v-\omega_0)\tau] = -(\partial/\partial\omega_0)\int d\tau\,\sin[(k_0 v-\omega_0)\tau]$.

Combining (1.11), (1.16) and (1.17) finally provides:

$$\begin{aligned}
\frac{d\,\mathrm{Kin}}{dt} &= -\frac{e}{2}E_0(t)\int dv\, v\, f_{10}(v)\sin[(k_0 v-\omega_0)t] \\
&\quad -\frac{e^2}{2m}E_0^2(t)\int dv\, v\,\frac{\partial f_0}{\partial v}\,\frac{\sin[(k_0 v-\omega_0)t]}{k_0 v-\omega_0} \\
&\quad -\frac{e^2}{4m}\frac{dE_0^2(t)}{dt}\frac{\partial}{\partial\omega_0}\int dv\, v\,\frac{\partial f_0}{\partial v}\,\frac{1-\cos[(k_0 v-\omega_0)t]}{k_0 v-\omega_0}.
\end{aligned}$$

In this last relation, one notes that the first term phase mixes to zero for times $t > 1/(k_0 v_{\mathrm{th}})$, where the thermal velocity v_{th} is the typical variation scale of the distribution in velocity. In the same time limit, one also has $\sin(\Omega t)/\Omega \to \pi\delta(\Omega)$ and $[1-\cos(\Omega t)]/\Omega \to P/\Omega$, where P stands for principal value, so that

$$\begin{aligned}
\frac{d\,\mathrm{Kin}}{dt} &= -\frac{e^2}{2m}E_0^2(t)\int dv\, v\,\frac{\partial f_0}{\partial v}\,\pi\delta(k_0 v-\omega_0) \;-\; \frac{e^2}{4m}\frac{dE_0^2(t)}{dt}\frac{\partial}{\partial\omega_0}\,P\!\!\int dv\,\frac{v\,\frac{\partial f_0}{\partial v}}{k_0 v-\omega_0} \\
&= \underbrace{-\pi\frac{\epsilon_0}{2}\frac{\omega_p^2}{k_0}E_0^2(t)\; v\,\frac{\partial f_0/N}{\partial v}\bigg|_{v=\omega/k_0}}_{\text{resonant}} \underbrace{-\;\frac{\epsilon_0}{4}\frac{dE_0^2(t)}{dt}\frac{\partial}{\partial\omega_0}\left[\omega_0\,\frac{\omega_p^2}{k_0^2}\,P\!\!\int dv\,\frac{\frac{\partial f_0/N}{\partial v}}{v-\omega_0/k_0}\right]}_{\text{bulk}},
\end{aligned} \tag{1.18}$$

where $\omega_p^2 = Ne^2/(m\epsilon_0)$ is the squared plasma frequency, and having used $\delta(k_0 v-\omega_0) = (1/k_0)\delta(v-\omega_0/k_0)$. The first term on the right hand side of Eq.(1.18) is clearly the contribution from the resonant particles with velocities matching the phase velocity $v_\phi = \omega_0/k_o$, while the second term corresponds to the contribution from the bulk of the distribution. In a sinusoidal wave with fixed amplitude, the bulk particles simply oscillate back and forth in the electrostatic field, and experience no secular gain or loss in energy. The resonant particles however experience a nearly constant field, and so can be efficiently accelerated or decelerated.

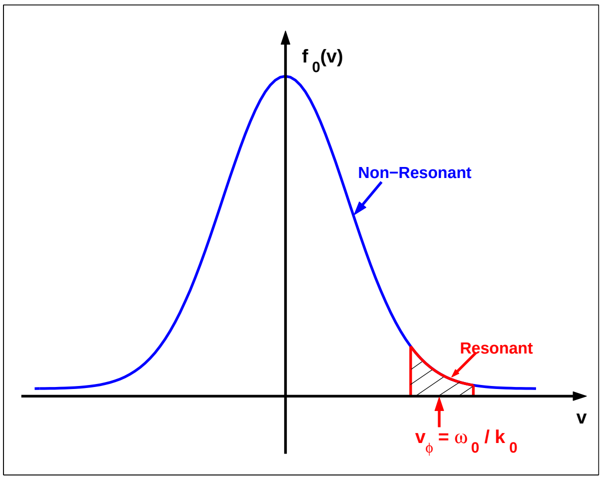

Figure 1.2: Separation of the distribution into a non-resonant and resonant part.

Invoking conservation of the total energy E_{tot}, the kinetic energy gained/lost by the particles must be compensated by the loss/gain of potential energy:

$$\frac{dE_{\text{tot}}}{dt} = \frac{d\,\text{Kin}}{dt} + \frac{d\text{Pot}}{dt} = 0, \tag{1.19}$$

where the space averaged potential energy Pot, i.e. the electrostatic energy, is given by

$$\text{Pot} = \langle \frac{\epsilon_0}{2} E^2(x,t) \rangle_x = \frac{\epsilon_0}{2} E_0^2(t) \, \langle \sin^2(k_0 x - \omega_0 t) \rangle_x = \frac{\epsilon_0}{4} E_0^2(t). \tag{1.20}$$

Combining (1.18), (1.19) and (1.20) leads to

$$\frac{\epsilon_0}{4} \frac{dE_0^2(t)}{dt} \frac{\partial}{\partial \omega_0} \left\{ \omega_0 \left[1 - \frac{\omega_p^2}{k_0^2} P\!\!\!\int dv \, \frac{\frac{\partial f_0/N}{\partial v}}{v - \omega_0/k_0} \right] \right\} = \pi \frac{\epsilon_0}{2} \frac{\omega_p^2}{k_0} E_0^2(t) \;\; v \left. \frac{\partial f_0/N}{\partial v} \right|_{v=v_\phi} . \tag{1.21}$$

On the right hand side of Eq.(1.21) one finds again the variation of kinetic energy of the resonant particles Kin^{res}, while on the left hand side one identifies the time variation of the wave energy E_{wave} (= bulk kinetic energy + Pot), given by the general relation:

$$E_{\text{wave}} = \text{Kin}^{\text{bulk}} + \text{Pot} = \frac{1}{4} \epsilon_0 \left. \frac{\partial}{\partial \omega} [\omega \, \epsilon_R(\omega)] \right|_{\omega_0} E_0^2(t), \tag{1.22}$$

where ϵ_R is the real, i.e. non-resonant, part of the media's dielectric function. Thus Eq.(1.21) reads

$$\frac{dE_{\text{wave}}}{dt} = -\frac{d\text{Kin}^{\text{res}}}{dt}. \tag{1.23}$$

For the Langmuir wave model considered here, with mobile electrons and fixed ions, one indeed has:

$$\epsilon_R(k,\omega) = 1 - \frac{\omega_p^2}{k^2} P\!\!\!\int dv \, \frac{\frac{\partial f_0/N}{\partial v}}{v - \omega/k}. \tag{1.24}$$

In the limit $v_\phi/v_{\rm th} \simeq 1/k_0\lambda_D \gg 1$, one can consider the cold fluid approximation $\epsilon_R = 1 - \omega_p^2/\omega^2$ of Eq.(1.24), so that $\partial(\omega\,\epsilon_R)/\partial\omega|_{\omega_0} \simeq 2$, as $\omega_0 \simeq \omega_p$.

Assuming an exponential decay of the wave:

$$E_0(t) = E_0\, e^{-\gamma_L t} \quad \Longrightarrow \quad \frac{d\,E_0^2(t)}{dt} = -2\gamma_L\, E_0^2(t),$$

one then recovers from Eq.(1.21) the well-known relation for the linear Landau damping (in the resonant approximation):

$$\gamma_L = -\frac{\pi}{2}\frac{\omega_p^2}{k_0}\, v\, \frac{\partial f_0/N}{\partial v}\bigg|_{v=v_\phi}. \tag{1.25}$$

In the case of a Maxwellian distribution $f_0(v) = N/(\sqrt{2\pi}v_{\rm th})\exp -v^2/(2v_{\rm th}^2)$, Eq.(1.25) becomes

$$\frac{\gamma_L}{\omega_0} = \sqrt{\frac{\pi}{8}}\frac{1}{(k_0\,\lambda_D)^3}\frac{\omega_0}{\omega_p}\exp -\frac{1}{2}\left(\frac{\omega_0}{k_0 v_{\rm th}}\right)^2. \tag{1.26}$$

Naturally, Eq.(1.25) leads to growth, i.e. instability, in case $v\partial f_0/\partial v|_{v=v_\phi} > 0$. This is the bump on tail instability.

Note that to re-derive the linear Landau damping relation (1.25) invoking energy conservation, one had to consider perturbation terms of the distribution up to second order, i.e. f_2. This is due to the fact that energy is intrinsically a non-linear quantity, as in particular the potential energy Pot is quadratic in the perturbation field, as appears clearly in Eq.(1.20).

Exercises:

1.2.2.1 Re-derive relation (1.25) for the linear Landau damping, starting from the linearized Vlasov-Poisson equations, computing the dispersion function $\epsilon(k,\omega)$, establishing the appropriate dispersion relation, and solving using the resonant approximation.

1.2.2.2 Derive the general relation (1.22) for the wave energy of an electrostatic wave. In fact, Eq. (1.22) can be further generalized to the case of an electromagnetic wave, for which:

$$E_{\rm wave} = \frac{1}{4}\left\{\epsilon_0\vec{E}_0 \cdot \frac{\partial}{\partial\omega}\left[\omega\,\epsilon_H(\omega)\right]\bigg|_{\omega_0} \cdot \vec{E}_0^\star + \frac{1}{\mu_0}\vec{H}_0 \cdot \frac{\partial}{\partial\omega}\left[\omega\,\mu_H(\omega)\right]\bigg|_{\omega_0} \cdot \vec{H}_0^\star\right\},$$

1.2.3 Limit of Linear Landau Damping

The derivation of the linear Landau damping presented in the previous section naturally breaks under conditions for which one reaches the limits of the considered perturbative approach. This is the case when $\partial f_1/\partial v$ becomes of the same order as $\partial f_0/\partial v$:

$$\text{Linear Landau damping derivation breaks down when} \quad \frac{\partial f_1}{\partial v} \sim \frac{\partial f_0}{\partial v}.$$

To estimate under which conditions this linear limit is met, one considers equation (1.15) for f_1. For our purpose here, one can neglect the time dependence of the field envelope, and thus directly carry out the remaining time integral in (1.15) to obtain:

$$f_1(x,v,t) = f_{10}(v)\cos[k_0(x-vt)] + \frac{e}{m}\frac{\partial f_0}{\partial v}E_0\frac{\cos[k_0(x-vt)] - \cos(k_0x-\omega_0 t)}{k_0v-\omega_0}. \quad (1.27)$$

Away from resonance ($\Omega = k_0v-\omega_0 \neq 0$), the derivative $\partial f_1/\partial v$ obviously produces secular terms, i.e. which grow linearly in time t. Near resonance, both the numerator and denominator in the second term on the right hand side of (1.27) go to zero, and so one must expand the numerator for small $\Omega = k_0v-\omega_0$ to address the variation of f_1 in this region. Noting that near resonance one has

$$\begin{aligned}
\cos[k_0(x-vt)] &= \cos[k_0x-\omega_0 t - \overbrace{(k_0v-\omega_0)}^{\Omega}\,t] \\
&= \cos(k_0x-\omega_0 t) + \sin(k_0x-\omega_0 t)\,(k_0v-\omega_0)t \\
&\quad -\frac{1}{2}\cos(k_0x-\omega_0 t)\,(k_0v-\omega_0)^2t^2 + \ldots,
\end{aligned}$$

equation (1.27) can be written in this region as

$$f_1(x,v,t) = f_{10}(v)\cos[k_0(x-vt)] + \frac{e}{m}\frac{\partial f_0}{\partial v}E_0\left[t\sin(k_0x-\omega_0 t) - \frac{1}{2}(k_0v-\omega_0)t^2\cos(k_0x-\omega_0 t) + \ldots\right]$$

The term in t^2 rapidly becomes dominant when estimating $\partial f_1/\partial v$:

$$\frac{\partial f_1}{\partial v} \simeq -\frac{1}{2}\frac{e}{m}\frac{\partial f_0}{\partial v}k_0E_0\,t^2\,\cos(k_0x-\omega_0 t),$$

so that

$$\text{At resonance:} \quad \frac{\partial f_1}{\partial v} \sim \frac{\partial f_0}{\partial v} \quad \Longleftrightarrow \quad t > \left(\frac{m}{ek_0E_0}\right)^{1/2} = \frac{1}{\omega_b}, \quad (1.28)$$

where $\omega_b^2 = ek_0E_0/m$. The frequency ω_b is identified as the bounce frequency of electrons deeply trapped in the potential wells of the wave. It is indeed important to note, that the electrons moving in the field $E = E_0\sin(k_0x-\omega_0 t)$ are separated into two groups: Passing and trapped. This is discussed in more detail in appendix A, where useful quantities such as ω_b are derived.

In the bulk of the distribution, i.e. away from resonance, one has $k_0v-\omega_0 \simeq -\omega_0$ and from Eq.(1.27):

$$\frac{\partial f_1}{\partial v} \simeq -\frac{e}{m}\frac{\partial f_0}{\partial v}k_0E_0\,t\,\frac{\sin[k_0(x-vt)]}{\omega_0},$$

so that

$$\text{In bulk:} \quad \frac{\partial f_1}{\partial v} \sim \frac{\partial f_0}{\partial v} \quad \Longleftrightarrow \quad t > \frac{m\omega_0}{ek_0E_0} = \frac{\omega_0}{\omega_b^2}, \quad (1.29)$$

Assuming $\omega_0 \gg \omega_b$, one sees from Eqs. (1.28) and (1.29) that the linear approximation breaks down much later in the bulk of the distribution than in the resonant region.

For the linear result, and in particular the handling of resonant particles, to be valid for describing the full evolution of the damping of the waves thus requires

$$\gamma_L > \omega_b. \tag{1.30}$$

Under this condition, the wave has indeed damped out before the linear approximation breaks down. For a given value of $k_0\lambda_D$, this last condition is equivalent to an upper limit on the amplitude of the wave, which can be written in the case of a Maxwellian distribution as:

$$\frac{\omega_b}{\omega_p} = \sqrt{\frac{\delta N}{N}} \quad < \quad \frac{\gamma_L}{\omega_p} \simeq \sqrt{\frac{\pi}{8}} \frac{1}{(k_0\lambda_D)^3} \exp\left[-\frac{1}{2}\frac{1}{(k_0\lambda_D)^2}\right], \tag{1.31}$$

where δN is the density perturbation amplitude of the Langmuir wave, and having used relation (1.26) for γ_L in the case of a Maxwellian plasma.

Exercises:

1.2.3.1 Show that for Langmuir waves one has the bounce frequency of deeply trapped electrons verifying $\omega_b/\omega_p = \sqrt{\delta N/N}$. Show also that the trapping width Δv_{trap} is such that $\Delta v_{\text{trap}} = 2\,\omega_b/k_0 \simeq 2\sqrt{\delta N/N}\, v_\phi$.

1.2.3.2 Verify the derivations in appendix A.

1.2.3.3 Draw the parallel between charged particles trapped in a sinusoidal electrostatic field, and particles trapped in the magnetic well of a large aspect ratio tokamak.

1.2.3.4 Show that the condition described by Eq. (1.30) is equivalent to imposing

$$\Delta\text{Kin} > E_{\text{wave}},$$

where ΔKin is the variation in kinetic energy which would result from flattening the electron distribution in the resonant region, and E_{wave} is the average wave energy of the Langmuir wave.

1.2.4 "Non-Linear Landau Damping"

In the previous section it was shown that the linear derivation of Landau damping is valid for describing the full collisionless attenuation of the wave in the limit $\omega_b \ll \gamma_L \ll \omega_0$. We shall now consider the case $\omega_b^2/\omega_0 \ll \gamma_L \ll \omega_b \ll \omega_0$. In this limit the trapped electrons have time to bounce back and forth many times in the potential wells of the electrostatic field $E(x,t)$ before the amplitude of the field is damped significantly. In this case, at least for the resonant particles, one must correctly account for the full non-linear trajectories of the electrons in the sinusoidal field $E = E_0 \sin(k_0 x - \omega_0 t)$. Note however, that according to Eq.(1.29), the scaling $\omega_b^2/\omega_0 \ll \gamma_L$ ensures that the linear response of the bulk distribution remains valid over the characteristic time scale of damping. Thus, the decomposition illustrated by Fig. 1.2 is still preserved, i.e. of a bulk, non-resonant distribution supporting, through a linear response, the oscillatory motion of the plasma wave (= dispersion), and of a relatively small fraction of resonant particles leading to damping/growth. As will appear clearly in the following, let us point out already that the effect of resonant particles include significant contributions from both the trapped electrons, as well as passing electrons near the separatrix shown in Fig. A.1.

The basic procedure for handling the non-linear evolution of the wave's amplitude is essentially the same as for the linear regime addressed in Sec. 1.2.2. Let us summarize. One again invokes total energy conservation by equating the rate of change of the wave energy E_{wave} to the variation of the kinetic energy of resonant particles Kin^{res}, as already written in Eq.(1.23):

$$\frac{dE_{\text{wave}}}{dt} = -\frac{d\text{Kin}^{\text{res}}}{dt}.$$

As just pointed out, the bulk of the distribution may still be assumed to respond linearly under the considered scaling, so that relation (1.22) for the wave energy still holds:

$$E_{\text{wave}} = \frac{1}{4}\epsilon_0 \left.\frac{\partial}{\partial\omega}\left[\omega\,\epsilon_R(\omega)\right]\right|_{\omega_0} E_0^2(t).$$

Recalling that for Langmuir waves one has $\partial(\omega\,\epsilon_R)/\partial\omega|_{\omega_0} \simeq 2$, and allowing for a time dependant damping/growth rate $\gamma(t)$ for the wave amplitude:

$$E_0(t) = E_0\, e^{-\int_0^t dt'\,\gamma(t')},$$

the rate of change of wave energy is thus again given by

$$\frac{dE_{\text{wave}}}{dt} = -\gamma(t)\epsilon_0\, E_0(t)^2. \tag{1.32}$$

Equation (1.8) for the variation of the kinetic energy of resonant particles is naturally still valid here:

$$\frac{d\,\text{Kin}^{\text{res}}}{dt} = \frac{m}{2}\int_{\text{res}} dv\, v^2 \langle\frac{\partial f}{\partial t}\rangle_x. \tag{1.33}$$

Thus from the above relations, the time dependant rate $\gamma(t)$ is computed from

$$\gamma(t) = \frac{1}{\epsilon_0 E_0^2}\frac{d\,\text{Kin}^{\text{res}}}{dt} = \frac{m}{2\epsilon_0 E_0^2}\int_{\text{res}} dv\, v^2 \langle\frac{\partial f}{\partial t}\rangle_x. \tag{1.34}$$

The non-linear calculation differs however from the linear case in the way the distribution f^{res} of resonant particles is computed. Indeed, here the distribution cannot be derived applying a perturbative approach as in Sec. 1.2.2, but must be calculated directly from the non-linear Vlasov equation:

$$\left.\frac{df}{dt}\right|_{\text{n.l.t.}} = \frac{\partial f}{\partial t} + v\frac{\partial f}{\partial x} - \frac{e}{m}E\,\frac{\partial f}{\partial v} = 0, \tag{1.35}$$

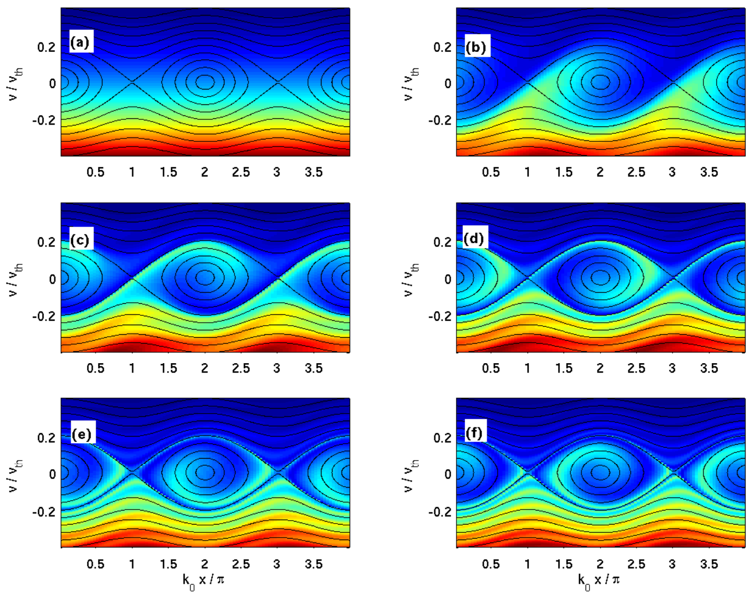

Figure 1.3: Evolution in resonant region of a Maxwellian distribution interacting with a sinusoidal wave. Results as seen from the wave frame. Black lines represent orbits of particles. Color coding reflects amplitude of distribution. Note how the density in phase space is preserved along the trajectories, but how the difference in the bounce/transit period between neighboring orbits leads to a filamentation of the distribution.

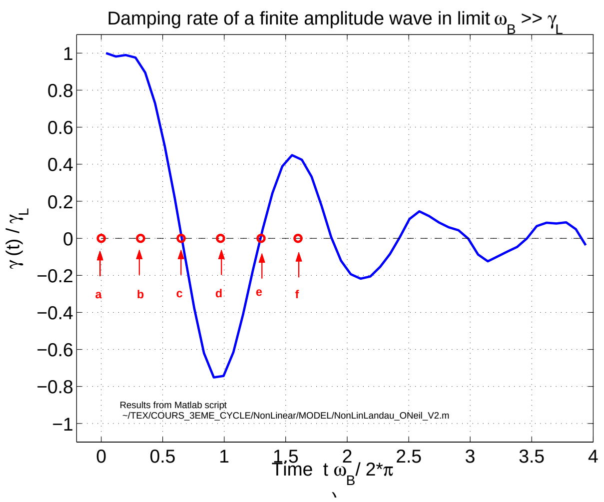

Figure 1.4: Instantaneous rate of change $\gamma(t)$ of wave amplitude as a function of time, as computed from Eq. (1.34). The rate $\gamma(t)$ is normalized with respect to the linear Landau damping rate γ_L, while time is given in units of the deeply trapped bounce period $\tau_b = 2\pi/\omega_b$. The rate $\gamma(t)$ reflects the change in kinetic energy of the resonant particles, as clearly illustrated by identifying the states of the distribution shown in Fig. 1.3 to the times a-f pointed out in this graph: At times when a majority of the resonant electrons are being accelerated (resp. decelerated), which corresponds to an increase (resp. decrease) in kinetic energy, one indeed observes positive damping (resp. negative damping = growth) of the wave.

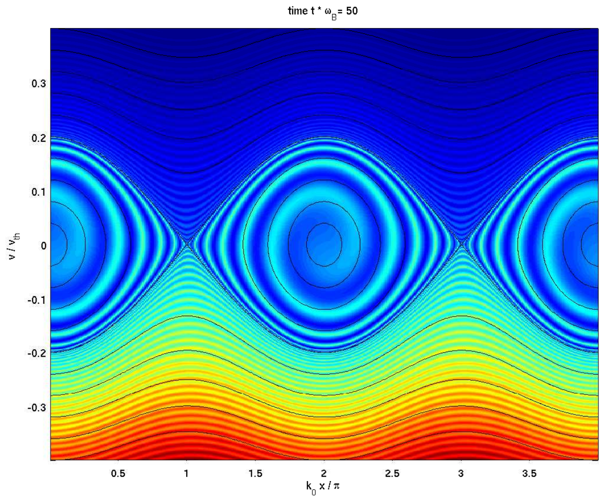

Figure 1.5: State of the distribution after $t\omega_b = 50$, clearly illustrating the increased filamentation in time of the distribution. At this stage, on average, the resonant particles are neither accelerated nor decelerated, and the rate of change $\gamma(t)$ of the wave amplitude becomes zero.

where $d/dt|_{\text{n.l.t.}}$ stands for the total time derivative along the non-linear trajectories, i.e. along the full characteristics in the electrostatic field E.

The Vlasov equation (1.35) can always be solved formally by integrating along the characteristics (see Appendix B):

$$f(x, v, t) = f[x'(0; x, v, t), v'(0; x, v, t), 0], \tag{1.36}$$

where $f(x, v, 0)$ is the initial distribution, and $[x'(t'; x, v, t), v'(t'; x, v, t)]$ the non-linear trajectories verifying:

$$\frac{dx'}{dt'} = v', \qquad \frac{dv'}{dt'} = -\frac{e}{m}E_0 \sin(k_0 x' - \omega_0 t'), \tag{1.37}$$

$$\text{with initial conditions} \quad x'(t) = x, \qquad v'(t) = v. \tag{1.38}$$

Note that one makes use of the time scale separation $\omega_b \gg \gamma_L$ by considering the amplitude E_0 of the field fixed when integrating the non-linear trajectories (1.37)-(1.38), which are then used for computing (1.36) and (1.34). The time dependence of $E_0(t)$ is then taken account for iteratively when computing dE_{wave}/dt through Eq. (1.32).

The above system of equations can easily be solved numerically, which provides a useful illustration of the mechanism underlying the non-linear evolution of the wave. This has been done to obtain the results presented in Figs. 1.3, 1.4 and 1.5.

Figures 1.3 and 1.4 show how the wave amplitude decreases $[\gamma(t) > 0]$ as a majority of the resonant particles are accelerated, which corresponds to an increase in kinetic energy. Inversely, the wave amplitude increases $[\gamma(t) < 0]$ as a majority of the resonant particles are decelerated, which corresponds to a decrease in kinetic energy. This is obviously the origin of the oscillations in kinetic and potential energy already observed in the full simulation results shown in Fig. 1.1.

According to the Vlasov equation, the density in phase space remains invariant along the trajectories of the particles. But as a result of the fact that neighboring orbits of passing particles (resp. trapped particles) have different transit times (resp. bounce periods), as shown in Fig. A.2, one observes a filamentation of the distribution over time. This is clearly illustrated in Fig. 1.5, which shows the distribution as computed from Eq.(1.36) at time $t\omega_b = 50$. At this stage, the resonant particles are neither accelerated nor decelerated on average, and the rate of change $\gamma(t)$ of the wave amplitude therefore tends to zero. As a result, the attenuation factor $\exp[-\int_0^\infty dt \gamma(t)]$ is non-zero, so that asymptotically in time one has an undamped mode. This resulting wave is a BGK mode. BGK modes are discussed in some detail in Sec. 1.2.5. As filamentation happens over the time scale of a few bounce periods ω_b, this phenomena is obviously only observed under the assumed scaling $\omega_b \gg \gamma$. Note the similarity between Figs. 1.3 & 1.5 and the phase space plots from the full simulations shown in Fig. 1.1.

The above system of equations (1.34), (1.36)-(1.38) can in fact also be solved analytically. The corresponding derivation, which is a somewhat lengthy exercise involving Jacobian elliptic functions [5], is described to some detail in Ref. [6]. From this derivation, the final result for the damping rate is

$$\gamma(t) = \gamma_L \sum_{n=0}^{\infty} \frac{64}{\pi} \int_0^1 d\kappa \, \{ \underbrace{\frac{2n\pi^2 \sin\left[\frac{n\pi\,\omega_b t}{\kappa F}\right]}{\kappa^5 F^2 (1+q^{2n})(1+q^{-2n})}}_{\text{passing}} + \underbrace{\frac{(2n+1)\pi^2 \kappa \sin\left[\frac{(2n+1)\pi\,\omega_b t}{2F}\right]}{F^2(1+q^{2n+1})(1+q^{-2n-1})}}_{\text{trapped}} \} \, , \tag{1.39}$$

where $q = \exp(\pi F'/F)$, $F = F(\kappa^2)$ is the complete elliptic integral of the first kind [5], and $F' = F'(\kappa^2) = F(1-\kappa^2)$. Equation (1.39) includes the integral $\int d\kappa$ over the energy variable κ, defined by (A.3), characterizing the different orbits of the resonant particles in phase space. The first term in the integrand corresponds to the contribution from the resonant passing particles, while the second term is related to trapped particles. Notice also the sum $\sum_n$ over harmonics of the transit period $\tau_t(\kappa) = 2\kappa F/\omega_b$ (resp. bounce period $\tau_b(\kappa) = 4F/\omega_b$) of passing (resp. trapped) particles. These relations for τ_t and τ_b for arbitrary energy levels κ are derived in Appendix A.

In the first stage of the evolution, that is in the limit $t \to 0$, one can show that Eq. (1.39) indeed recovers the linear damping rate $\gamma(t) \to \gamma_L$, as illustrated in Fig. 1.4. One needs to be careful however in taking this limit, as this is a typical case where $\lim_{t\to 0} \int d\kappa \neq \int d\kappa \lim_{t\to 0}$.

Due to the dependence in κ of τ_t and τ_b, as shown in Fig. A.2, one can see that the integrals in κ over the terms $\sin[n\pi\,\omega_b\, t/\kappa F]$ and $\sin[(2n+1)\pi\,\omega_b t/2F]$ phase mix to zero

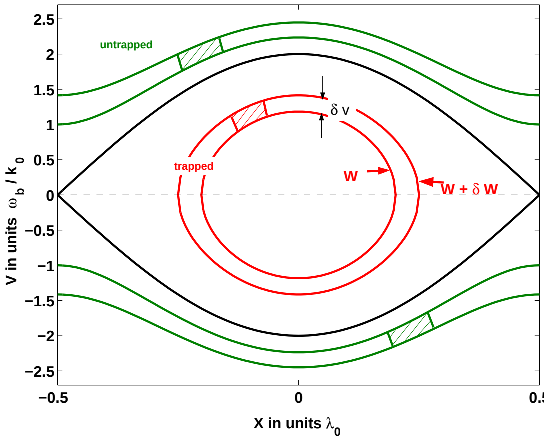

Figure 1.6: Initial sub-volumes in phase space within the region limited by orbits with energy levels W and $W = \delta W$ for both passing and trapped particles. In time, due to the difference in periods of the neighboring trajectories, these sub-volumes are stretched into ever finer filaments that ultimately uniformly fill the full volume between the two orbits.

as t becomes large, and thus one can show that $\lim_{t\to\infty} \gamma(t) = 0$. This can also be seen in Fig. 1.4.

The full derivation of Eq.(1.39) is not presented here. However, a direct calculation of the time integrated damping exponent $\int_0^\infty dt\, \gamma(t)$, which is perhaps one of the most useful results, is now carried out. From Eq.(1.34) one can write:

$$\int_0^\infty dt\, \gamma(t) = \frac{1}{\epsilon_0 E_0^2}\, \Delta\mathrm{Kin}^{\mathrm{res}}, \tag{1.40}$$

where

$$\Delta\mathrm{Kin}^{\mathrm{res}} = \frac{m}{2\lambda_0} \int_{-\lambda_0/2}^{\lambda_0/2} dX \int_{\mathrm{res}} dV\, (V + v_\phi)^2 (f_\infty - f_0), \tag{1.41}$$

$f_0 = f(X, V, t = 0)$ and $f_\infty = f(X, V, t = \infty)$ being respectively the initial and time asymptotic distribution in wave frame variables ($X = x - v_\phi t, V = v - v_\phi$). For convenience, the following derivation is indeed carried out in wave frame variables. However, to lighten notations one reverts to the notation (x, v) for position and velocity in the wave frame.

The main issue here is to evaluate $f_\infty(x, v)$. For this purpose, let us analyze in somewhat more detail the mechanism of filamentation. Figure 1.6 shows in the wave frame a small compact sub-volume in phase space within the region limited by orbits with energy levels W and $W + \delta W$, both for the case of trapped, as well as forward/backward passing particles. In all cases, the difference in periods of the trajectories with energies between W and $W + \delta W$ leads to a stretching over time of the sub-volume into an ever finer filament that ultimately evenly fills the whole region between the two orbits. As a result of the incompressibility of phase space, the density f remains invariant between the initial and final stretched state of the sub-volume. This stretching obviously happens for all the other initially compact sub-volumes within the orbits W and $W + \delta W$, so that asymptotically in time all these sub-volumes are finely intertwined with each other. This effect is clearly illustrated in Fig. 1.5. The coarse grain distribution $\hat{f}$ obtained by averaging the actual distribution f over phase elements sufficiently large to be crossed by many of these filaments thus becomes uniform within the orbits W and $W+\delta W$ and corresponds to the average of the initial distribution f_0 within these two orbits. Obviously, the size of the coarse-graining for computing $\hat{f}$ can be taken to zero asymptotically in time.

Note, that in a real physical system, even with very low collisionality, these ever finer phase space structures in fact always end up getting smeared out in a finite time through collisional diffusion. Indeed, for a given collisionality ν_c, a structure in the distribution with scale λ_v in velocity diffuses in a characteristic time $t_c \sim \nu_c^{-1}(\lambda_v/v_{\rm th})^2$.

On the basis of the above arguments, the distribution for untrapped particles [$W > \max(-e\phi)$] is obtained asymptotically in time from

$$f^{\rm u}_\infty(W,\sigma) = \hat{f}_\infty = \frac{\int_{-\lambda_0/2}^{\lambda_0/2} dx\, \delta v(x,W)\, f_0[\sigma v(x,W)]}{\int_{-\lambda_0/2}^{\lambda_0/2} dx\, \delta v(x,W)},$$

where the initial distribution f_0 is in fact only function of velocity v. In the above relation, $\sigma = \mathrm{sign}(v)$, $v(x,W)$ is the velocity at point x of the trajectory with energy W, by convention chosen positive, and $\delta v(x,W)$ the separation in velocity between orbits W and $W+\delta W$. Note that for untrapped particles each energy level W corresponds to both a forward passing ($\sigma = +1$) as well as a backward passing ($\sigma = -1$) trajectory, which must in general be treated separately. From energy conservation for a single particle, one has

$$\begin{aligned} \frac{1}{2}mv^2 - e\phi(x) = W \qquad &\Longrightarrow \qquad v(x,W) = \left[\frac{2}{m}(W+e\phi)\right]^{1/2} \\ &\Longrightarrow \qquad \delta v(x,W) = \frac{\partial v}{\partial W}\,\delta W = \frac{\delta W}{m\, v(x,W)}. \end{aligned}$$

The asymptotic untrapped distribution thus can be written

$$f^{\rm u}_\infty(W,\sigma) = \frac{\int_{-\lambda_0/2}^{\lambda_0/2} f_0[\sigma v(x,W)]\, dx/v(x,W)}{\int_{-\lambda_0/2}^{\lambda_0/2} dx/v(x,W)}. \tag{1.42}$$

For trapped particles [$\min(-e\phi) < W < \max(-e\phi)$] each energy level W represents a single orbit, which includes however both a forward as well as a backward going segment, so that for this group of particles the asymptotic distribution is computed from

$$f^{\rm t}_\infty(W) = \hat{f}_\infty = \frac{\sum_{\sigma=\pm 1}\int_{x_1}^{x_2} f_0[\sigma v(x,W)]\, dx/v(x,W)}{2\int_{x_1}^{x_2} dx/v(x,W)}. \tag{1.43}$$

where $x_{1,2}$ are the turning points, i.e. where $v(x_{1,2}, W) = 0$.

As the time asymptotic distributions (1.42) and (1.43) are to be used for computing the variation in kinetic energy (1.41) of the resonant particles, the distribution f_0 in (1.42) and (1.43) can be Taylor-expanded around the wave phase velocity, which in the wave frame is $v = 0$. This naturally assumes that the resonant region, of the order Δv_{trap}, is such that $\Delta v_{\text{trap}}/v_{\text{th}} \ll 1$. For the purpose of computing $\Delta\text{Kin}^{\text{res}}$, the leading order effect is obtained by considering a Taylor expansion to first order:

$$f_0(v) = f_0(0) + \frac{df_0(0)}{dv}\, v + \dots. \tag{1.44}$$

Inserting (1.44) in (1.42) thus leads to

$$f^{\text{u}}_{\infty}(W, \sigma) = f_0(0) + \frac{df_0(0)}{dv} \frac{\sigma \int_{-\lambda_0/2}^{\lambda_0/2} dx}{\int_{-\lambda_0/2}^{\lambda_0/2} dx/v(x, W)} + \dots = f_0(0) + \frac{df_0(0)}{dv}\, \frac{\sigma\lambda_0}{\tau_t} + \dots,$$

where τ_t stands for the transit time. Restricting the derivation to sinusoidal waves, one makes use of Eq. (A.4) to obtain:

$$f^{\text{u}}_{\infty}(\kappa, \sigma) = f_0(0) + \frac{df_0(0)}{dv}\, \sigma \frac{\pi}{2} \frac{\Delta v_{\text{trap}}}{\kappa\, F(\kappa^2)} + \dots,$$

so that together with (1.44):

$$\Delta f^{\text{u}} = f^{\text{u}}_{\infty} - f^{\text{u}}_{0} = \frac{df_0(0)}{dv} \left(\sigma \frac{\pi}{2} \frac{\Delta v_{\text{trap}}}{\kappa\, F(\kappa^2)} - v \right) + \dots. \tag{1.45}$$

For trapped particles, the term in df_0/dv obviously cancels out:

$$f^{\text{t}}_{\infty}(W) = f_0(0) + \frac{df_0(0)}{dv} \frac{\sum_{\sigma=\pm 1} \sigma \int_{x_1}^{x_2} dx}{2 \int_{x_1}^{x_2} dx/v(x, W)} + \dots = f_0(0) + \dots,$$

so that

$$\Delta f^{\text{t}} = f^{\text{t}}_{\infty} - f^{\text{t}}_{0} = -\frac{df_0(0)}{dv}\, v + \dots. \tag{1.46}$$

To the considered order, $\Delta f = f_{\infty} - f_0$ is clearly odd in v, so that Eq.(1.41) can be written

$$\Delta\text{Kin}^{\text{res}} = \frac{2m\, v_{\phi}}{\lambda_0} \int_{-\lambda_0/2}^{\lambda_0/2} dx \int_0^{\infty} dv\, v\, \Delta f. \tag{1.47}$$

Note, that although one is only computing the resonant particle contribution to $d\text{Kin}/dt$, the integration in velocity has been prolonged here to infinity. This is justified by proving that the relation Δf^{u} for passing particles derived in Eq. (1.45) actually goes to zero for $v \to \infty$ ($\kappa \to 0$), and in this way the velocity integral in (1.47) finds its own cutoff (check it!).

By making the change of variables $v \leftrightarrow \kappa$, so that from Eq.(A.2) $dv = \Delta v_{\rm trap}^2/(v\kappa^3)\, d\kappa$, one can write:

$$\Delta{\rm Kin}^{\rm res} = 2m\, v_\phi\, \Delta v_{\rm trap}^2 \left[\underbrace{\int_0^1 \frac{d\kappa}{\kappa^3}\frac{1}{\lambda_0}\int_{-\lambda_0/2}^{\lambda_0/2} dx\, \Delta f^{\rm u}}_{\rm passing} + \underbrace{\int_1^\infty \frac{d\kappa}{\kappa^3}\frac{1}{\lambda_0}\int_{x_1}^{x_2} dx\, \Delta f^{\rm t}}_{\rm trapped} \right], \tag{1.48}$$

where the first term in (1.48) corresponds to the contribution from untrapped electrons, and the second term to trapped. Expliciting the space integral for passing particles leads to

$$\begin{aligned} \frac{1}{\lambda_0}\int_{-\lambda_0/2}^{\lambda_0/2} dx\, \Delta f^{\rm u} &= \frac{df_0(0)}{dv}\left[\frac{\pi}{2}\frac{\Delta v_{\rm trap}}{\kappa\, F(\kappa^2)} - <v>_x\right] \\ &= \frac{df_0(0)}{dv}\frac{\Delta v_{\rm trap}}{\kappa}\left[\frac{\pi}{2\, F(\kappa^2)} - \frac{2\, E(\kappa^2)}{\pi}\right], \end{aligned} \tag{1.49}$$

having made use of Eq. (1.45) for $\Delta f^{\rm u}$ and Eq. (A.5) for the spatial averaged velocity $<v>_x$. The corresponding integral for trapped particles becomes:

$$\begin{aligned} \frac{1}{\lambda_0}\int_{x_1}^{x_2} dx\, \Delta f^{\rm t} &= -\frac{df_0(0)}{dv} <v>_x \\ &= -\frac{df_0(0)}{dv}\frac{2\Delta v_{\rm trap}}{\pi}\left[E(\frac{1}{\kappa^2}) + (\frac{1}{\kappa^2}-1)F(\frac{1}{\kappa^2})\right], \end{aligned} \tag{1.50}$$

having made use of Eq. (1.46) for $\Delta f^{\rm t}$ and Eq. (A.7) for $<v>_x$.

Inserting Eqs. (1.49) and (1.50) into (1.48) then provides

$$\begin{aligned} \Delta{\rm Kin}^{\rm res} &= 4m\, v_\phi\, \Delta v_{\rm trap}^3 \frac{df_0(0)}{dv}\left\{\int_0^1 \frac{d\kappa}{\kappa^4}\left[\frac{\pi}{4\, F(\kappa^2)} - \frac{E(\kappa^2)}{\pi}\right] - \int_1^\infty \frac{d\kappa}{\kappa^3}\frac{1}{\pi}\left[E(\frac{1}{\kappa^2}) + (\frac{1}{\kappa^2}-1)F(\frac{1}{\kappa^2})\right]\right\} \\ &= \frac{\gamma_L}{\omega_b}\,\epsilon_0 E_0^2\, \frac{64}{\pi}\int_0^1 d\kappa \left\{\frac{1}{\kappa^4}\left[\frac{E(\kappa^2)}{\pi} - \frac{\pi}{4\, F(\kappa^2)}\right] + \frac{\kappa}{\pi}\left[E(\kappa^2) + (\kappa^2-1)F(\kappa^2)\right]\right\}, \end{aligned} \tag{1.51}$$

having made the change of variable $\kappa \to 1/\kappa$ for the trapped contribution, and made use of Eq. (1.25) for the linear Landau damping γ_L.

Finally, inserting (1.51) in (1.40) leads to:

$$\int_0^\infty dt\, \gamma(t) = \frac{\gamma_L}{\omega_b}\frac{64}{\pi}\int_0^1 d\kappa \left\{ \underbrace{\frac{1}{\kappa^4}\left[\frac{E(\kappa^2)}{\pi} - \frac{\pi}{4\, F(\kappa^2)}\right]}_{\rm passing} + \underbrace{\frac{\kappa}{\pi}\left[E(\kappa^2) + (\kappa^2-1)F(\kappa^2)\right]}_{\rm trapped} \right\}. \tag{1.52}$$

Note how this result scales as γ_L/ω_b, which is assumed small in the considered ordering. Recall that for a Maxwellian, γ_L/ω_p is essentially a function of $k\lambda_D$ [see Eq.(1.26)], while $\omega_b/\omega_p = \sqrt{\delta N/N}$.

In the constant factor on the right hand side of Eq. (1.52), one can still distinguish the contribution of untrapped (first term) from the one of trapped particles (second term). By numerical integration, this constant can be estimated: $(64/\pi)\int_0^1 d\kappa \ldots \simeq 1.96$, with the contribution from untrapped particles being 0.52 and from trapped 1.44.

Exercises:

1.2.4.1 Recover (1.52) from (1.39) making use of the following relations:

$$\begin{aligned} \frac{2\pi}{F(\kappa^2)} \sum_{n=1}^{\infty} \frac{1}{(1+q^{2n})(1+q^{-2n})} &= \frac{E(\kappa^2)}{\pi} - \frac{\pi}{4\,F(\kappa^2)}, \\ \frac{2\pi^2}{\kappa^2\,F(\kappa^2)} \sum_{n=1}^{\infty} \frac{1}{(1+q^{2n-1})(1+q^{-2n+1})} &= \left(1-\frac{1}{\kappa^2}\right) F(\kappa^2) + \frac{1}{\kappa^2} E(\kappa^2). \end{aligned}$$

1.2.4.2 Compare the "exact" non-linear simulation results shown in Fig. 1.1 to the analytic relations (1.39) and (1.52). Is there qualitative agreement? Quantitative agreement? Recall that the simulation results in figure 1.1 are for standing Langmuir waves.

1.2.5 BGK waves

From the previous section, where the regime $\gamma_L \ll \omega_b$ has been studied, it appears that the non-linear evolution of a Langmuir wave leads, asymptotically in time, towards a finite amplitude, undamped mode. Let us now see in more detail how such a state is characterized. In fact, one wants to further convince oneself that such an undamped mode can actually exist as an exact self-consistent solution of the non-linear Vlasov-Poisson system.

In the wave frame, an undamped mode corresponds to a stationary solution of the Vlasov-Poisson system. Such a state is thus characterized by a time independent distribution $f = f(x, v)$ for each species, and a time independent potential field $\phi = \phi(x)$. The distribution f for each species, with charge q and mass m, is solution to the corresponding stationary Vlasov equation:

$$\left[v\frac{\partial}{\partial x} - \frac{q}{m}\frac{d\phi(x)}{dx}\frac{\partial}{\partial v}\right] f(x, v) = 0.$$

As a result, f must be a function of the invariants of motion. For particles trapped in the troughs of the potential ϕ, the only conserved quantity is the total energy $W = mv^2/2 + q\phi(x)$, while for untrapped particles the sign σ of the velocity is an additional invariant. The stationary distribution must therefore be of the form:

$$f(x, v) = f(W, \sigma) = f^{\mathrm{t}}(W) + f^{\mathrm{u}}(W, \sigma), \tag{1.53}$$

where $f^{\rm t}(W)$ is the distribution of trapped particles, non-zero for $\min(q\phi) < W < \max(q\phi)$, and $f^{\rm u}(W,\sigma)$ is the distribution of untrapped particles, non-zero for $W > \max(q\phi)$.

The potential $\phi(x)$ is solution of Poisson's equation:

$$
\begin{aligned}
\frac{d^2\phi(x)}{dx^2} &= -\frac{1}{\epsilon_0}\sum_{\text{species}} q \int_{-\infty}^{+\infty} dv\, f(x,v) \\
&= -\frac{1}{\epsilon_0}\sum_{\text{species}} q \int_{-\infty}^{+\infty} dv\, f(W = mv^2/2 + q\,\phi(x), \sigma) \\
&= -\frac{1}{\epsilon_0}\sum_{\text{species}} q \int_{q\phi}^{\infty} \frac{dW\, \sum_{\sigma=\pm 1} f(W,\sigma)}{[2m(W-q\phi)]^{1/2}}.
\end{aligned}
\tag{1.54}
$$

Thus, in principal, given any distribution of the form (1.53), Eq. (1.54) defines a second order ordinary differential equation (ODE) for $\phi(x)$. The so-obtained set $[\{f\}_{\text{species}}, \phi]$ corresponds to a non-linear, undamped state. Such undamped states are the so-called Bernstein-Greene-Kruskal (BGK) modes [7].

Note from Eq. (1.54), that the potential $\phi(x)$ in fact depends only on $\sum_{\sigma=\pm 1} f(W,\sigma)$. As a result, $\phi(x)$ remains invariant if one varies the partition between forward and backward passing particles while keeping $\sum_{\sigma=\pm 1} f(W,\sigma)$ unchanged. Thus, for a given ϕ one can arbitrarily vary the phase velocity in the lab frame (defined as the frame in which the system has zero average momentum).

Equation (1.54) can be written as

$$
\frac{d^2\phi(x)}{dx^2} = F(\phi), \tag{1.55}
$$

where $F(\phi)$ is the right hand side of (1.54), and can be viewed as the "force" acting on a "particle" with "position" ϕ and evolving in "time" x. By multiplying Eq.(1.55) by $d\phi/dx$ and integrating in x, one thus obtains

$$
\frac{1}{2}(\frac{d\phi}{dx})^2 + V(\phi) = \text{const.}, \tag{1.56}
$$

where the "potential" $V(\phi)$ is such that $dV(\phi)/d\phi = -F(\phi)$, and is given by

$$
V(\phi) = -\frac{1}{\epsilon_0}\sum_{\text{species}} \int_{q\phi}^{\infty} dW \left[\frac{2}{m}(W - q\phi)\right]^{1/2} \sum_{\sigma=\pm 1} f(W,\sigma).
$$

Obviously, if $V(\phi)$ has a minimum, one can obtain periodic solutions for $\phi(x)$.

Equation (1.56) can be solved by quadrature:

$$
\pm\int_{\phi_0}^{\phi} \frac{d\phi}{\left[2\left(V(\phi_0) - V(\phi)\right)\right]^{1/2}} = x - x_0
$$

where the "initial conditions" have been chosen such that at position $x = x_0$ one has $\phi(x_0) = \phi_0$ and $d\phi(x_0)/dx = 0$.

Inversely, one can demonstrate [7] that from any given potential field $\phi(x)$ and given distributions for the various species (electrons and ions) and groups (passing and trapped), except one (e.g. the distribution $f_e^t(W)$ of trapped electrons), one can build a BGK-type mode by solving for this undetermined distribution.

Thus, it obviously appears that one can build BGK modes of quite arbitrary shape of the potential $\phi(x)$ and in particular wavelength. Furthermore, as already pointed out, for a given ϕ the wave velocity in the lab frame can also be chosen arbitrarily. Hence, in general, the wave numbers and frequencies of BGK modes do not need to obey the dispersion relations derived in the framework of linear theory. The larger this deviation from the linear dispersion relation, the stronger the distribution of the BGK mode must be deformed from the initial, unperturbed equilibrium distribution (usually a Maxwellian) considered in linear theory. To reach a state which is far from equilibrium naturally requires the system to be very strongly driven.

1.2.6 Non-Linear Frequency Shift

In Sec. 1.2.4, the non-linear evolution of the *amplitude* of a Langmuir wave was studied in the regime $\omega_b^2/\omega_0 \ll \gamma_L \ll \omega_b \ll \omega_0$. It was shown how such a wave ultimately evolves towards a finite amplitude, undamped mode, a so-called BGK mode. The characteristics of these BGK modes were discussed in Sec. 1.2.5, and it was pointed out how in general they do not necessarily obey the dispersion relations from linear theory. In the case of interest in section 1.2.4, let us recall however that the assumed scaling ensures that the main part of the distribution, the so-called bulk, still responds linearly. One therefore expects in this case, that the frequency and wavelength of the final BGK state verify a dispersion relation which corresponds to the linear one with at most a small correction due to the minority fraction of non-linearly behaving resonant particles. The purpose of this section is to derive this non-linear correction. Note that the evolution of the electron plasma wave considered in 1.2.4 is an initial value problem, for which the fundamental wavenumber k_0 remains fixed. A non-linear correction to the dispersion relation will thus affect the frequency, i.e. potentially leading to a non-linear frequency shift.

One starts from Poisson's equation for the potential ϕ of the final, BGK-like state of the electron plasma wave considered in Sec. 1.2.4, i.e. a case with dynamic electrons and a fixed, neutralizing ion background:

$$\frac{d^2\phi}{dx^2} = \frac{1}{\epsilon_0}\left[e\int_{-\infty}^{+\infty} dv\, f_\infty - q_i N_{i,0}\right], \tag{1.57}$$

where f_∞ is the time asymptotic distribution given by Eqs. (1.42) and (1.43) for passing and trapped particles respectively, q_i is the charge of ions and $N_{i,0}$ their uniform density.

To explicit the purely non-linear response, one adds and subtracts in (1.57) the charge density related to the linear response of the system:

$$\begin{aligned}
\frac{d^2\phi}{dx^2} &= \frac{1}{\epsilon_0}\left[e\int_{-\infty}^{+\infty} dv\, f_{\mathrm{L}} - q_i N_{i,0} + e\int_{-\infty}^{+\infty} dv\,(f_\infty - f_{\mathrm{L}})\right] \\
&= \frac{e}{\epsilon_0}\left[\int_{-\infty}^{+\infty} dv\ \delta f + \int_{-\infty}^{+\infty} dv\,(f_\infty - f_{\mathrm{L}})\right], \qquad (1.58)
\end{aligned}$$

where $f_L = f_0 + \delta f$, f_0 being the initial unperturbed electron distribution verifying the neutrality condition $e\int dv f_0 = q_i N_{i,0}$, and δf the actual linear perturbation. For a wave with wave number k and frequency ω in the lab frame, one has

$$\delta f = -\frac{e}{m}\frac{k\phi}{kv-\omega}\frac{\partial f_0}{\partial v}, \qquad (1.59)$$

which is obtained from the linearized Vlasov equation:

$$\frac{\partial \delta f}{\partial t} + v\frac{\partial \delta f}{\partial x} + \frac{e}{m}\frac{\partial \phi}{\partial x}\frac{\partial f_0}{\partial v} = 0.$$

Inserting (1.59) in (1.58), and making use of the fact that the wave remains mainly sinusoidal with wave number k_0, enables to write:

$$-k_0^2\,\epsilon_L(k_0,\omega)\phi = \frac{e}{\epsilon_0}\int_{-\infty}^{+\infty} dv\,\Delta f_{\mathrm{NL}}, \qquad (1.60)$$

having defined the non-linear deviation of the distribution $\Delta f_{\mathrm{NL}} = f_\infty - f_{\mathrm{L}}$. In equation (1.60) $\epsilon_L(k,\omega)$ is the linear dielectric function

$$\epsilon_{\mathrm{L}}(k,\omega) = 1 - \frac{\omega_p^2}{k^2}\int dv \frac{\frac{\partial f_0/N}{\partial v}}{v-\omega/k}.$$

The non-linear charge density on the right hand side of Eq. (1.60) appears as an external source term to a system responding linearly with dielectric ϵ_L.

One now projects Eq. (1.60) onto ϕ, i.e. carries out $\langle\phi\ldots\rangle_x = (1/\lambda_0)\int_{-\lambda_0/2}^{\lambda_0/2} dx\,\phi\ldots$ on each side of the equation, to obtain:

$$\begin{aligned}
\epsilon_L(k_0,\omega) &= -\frac{2}{\epsilon_0 E_0^2}\frac{1}{\lambda_0}\int_{-\lambda_0/2}^{\lambda_0/2} dx\, e\phi\int_{-\infty}^{+\infty} dv\,\Delta f_{\mathrm{NL}} \\
&= -\frac{2}{\epsilon_0 E_0^2}\frac{1}{\lambda_0}\int_{-\lambda_0/2}^{\lambda_0/2} dx\, e\phi\int_{-e\phi}^{+\infty}\frac{dW}{mv(x,W)}\sum_{\sigma=\pm1}\Delta f_{\mathrm{NL}}, \qquad (1.61)
\end{aligned}$$

having used $\langle\phi^2\rangle_x = E_0^2/(2k_0^2)$. To obtain the last equality in (1.61) one has changed to wave frame variables, and made a variables transformation from velocity v to wave frame energy $W = mv^2/2 - e\phi$, so that $v(x, W) = +[(2/m)(W + e\phi(x))]^{1/2}$. As will clearly appear in the following, this change of frame and variables is convenient for expliciting $\Delta f_{\rm NL} = f_\infty - f_{\rm L}$.

The distribution f_∞ is given in wave frame variables by Eqs. (1.42) and (1.43) for passing and trapped particles respectively. As appears from (1.61), it is in fact $\sum_{\sigma=\pm 1} f_\infty$ which is required. This quantity can actually be represented for both groups of particles, passing and trapped, by the single, compact relation:

$$
\begin{aligned}
\sum_{\sigma=\pm 1} f_\infty(W, \sigma) &= \frac{\sum_\sigma \int_{-\lambda_0/2}^{\lambda_0/2} dx f_0[\sigma v(x, W)] \, \frac{H(W+e\phi)}{v(x,W)}}{\int_{-\lambda_0/2}^{\lambda_0/2} dx \, \frac{H(W+e\phi)}{v(x,W)}} \\
&= \frac{\sum_\sigma \langle f_0[\sigma v(x, W)] \frac{H(W+e\phi)}{v(x,W)} \rangle_x}{\langle \frac{H(W+e\phi)}{v(x,W)} \rangle_x},
\end{aligned} \tag{1.62}
$$

where $H(w)$ is the Heaviside step function, defined as $H(w) = 0$ for $w < 0$, and $H(w) = 1$ for $w > 0$.

One expects the non-linear deviation $\Delta f_{\rm NL}$ to be essentially non-zero in the resonant region, i.e. around $v = 0$ in the wave frame. Thus, as in section 1.2.4 for addressing the non-linear damping, one can here again Taylor-expand f_0 around $v = 0$. However, as a result of the summing over $\sigma = \pm 1$, which cancels out the first order terms, the expansion must be considered in this case to second order:

$$
f_0(v) = f_0(0) + \frac{df_0(0)}{dv} v + \frac{1}{2} \frac{d^2 f_0(0)}{dv^2} v^2 + \ldots . \tag{1.63}
$$

Inserting (1.63) in (1.62) provides:

$$
\sum_{\sigma=\pm 1} f_\infty(W, \sigma) = 2f_0(0) + \frac{d^2 f_0(0)}{dv^2} \frac{\langle H v(x, W) \rangle_x}{\langle \frac{H}{v(x,W)} \rangle_x} + \ldots \simeq 2f_0(0) + \frac{d^2 f_0(0)}{dv^2} \frac{\bar{v}}{m\bar{v}'}, \tag{1.64}
$$

having used the notation $\bar{v} = \langle H v \rangle_x$ for the average velocity and $\bar{v}' = d\bar{v}/dW = (1/m)\langle H/v(x, W) \rangle_x$. Naturally, H is the shorter notation for $H(W + e\phi)$.

The linear distribution $f_{\rm L} = f_0 + \delta f$ is also expanded up to order $d^2 f_0/dv^2$, so that using (1.59) in wave frame variables one obtains:

$$
\begin{aligned}
\sum_{\sigma=\pm 1} f_{\rm L} &= \sum_\sigma \left[f_0(v) - \frac{e}{m} \frac{\phi}{v} \frac{df_0(v)}{dv} \right] \\
&\simeq \sum_\sigma \left\{ f_0(0) + \frac{df_0(0)}{dv} v + \frac{1}{2} \frac{d^2 f_0(0)}{dv^2} v^2 - \frac{e}{m} \frac{\phi}{v} \left[\frac{df_0(0)}{dv} + \frac{d^2 f_0(0)}{dv^2} v \right] \right\} \\
&= 2f_0(0) + \frac{d^2 f_0(0)}{dv^2} \left(v^2 - 2\frac{e\phi}{m} \right) = 2f_0(0) + \frac{d^2 f_0(0)}{dv^2} \frac{2}{m} W.
\end{aligned} \tag{1.65}
$$

Combining (1.64) and (1.65) thus provides

$$\sum_{\sigma=\pm 1} \Delta f_{\mathrm{NL}} = \sum_{\sigma}(f_{\infty} - f_{\mathrm{L}}) \simeq \frac{d^2 f_0(0)}{dv^2}\left(\frac{\bar{v}}{m\bar{v}'} - \frac{2}{m}W\right) = -\frac{2}{m\bar{v}'}\frac{d^2 f_0(0)}{dv^2}(W\bar{v}' - \frac{\bar{v}}{2}). \quad (1.66)$$

Figure 1.7 shows the distributions $\sum_\sigma f_\infty$ and $\sum_\sigma f_{\mathrm{L}}$ in the resonant region.

The above relation derived for $\sum_\sigma \Delta f_{\mathrm{NL}}$ is clearly only function of W, so that in Eq.(1.61) one can invert the integrals over x and W as follows:

$$\begin{aligned}
\epsilon_L(k_0,\omega) &= -\frac{2}{\epsilon_0 E_0^2}\int_{\min(-e\phi)}^{+\infty} dW \sum_\sigma \Delta f_{\mathrm{NL}}\, \frac{1}{\lambda_0}\int_{-\lambda_0/2}^{\lambda_0/2} dx\, \frac{e\phi\; H(W+e\phi)}{m\, v(x,W)} \\
&= \frac{2}{\epsilon_0 E_0^2}\int_{\min(-e\phi)}^{+\infty} dW\,(W\bar{v}' - \frac{\bar{v}}{2}) \sum_\sigma \Delta f_{\mathrm{NL}},
\end{aligned} \quad (1.67)$$

having used

$$\begin{aligned}
\frac{1}{\lambda_0}\int_{-\lambda_0/2}^{\lambda_0/2} dx\, \frac{e\phi\, H(W+e\phi)}{mv(x,W)} &= \frac{1}{\lambda_0}\int_{-\lambda_0/2}^{\lambda_0/2} dx\, \frac{-(W - mv^2/2)\, H(W+e\phi)}{mv} \\
&= -\frac{W}{m}\langle\frac{H}{v}\rangle_x + \frac{1}{2}\langle Hv\rangle_x = -(W\bar{v}' - \frac{\bar{v}}{2}).
\end{aligned}$$

Inserting (1.66) into (1.67) thus gives

$$\epsilon_L(k_0,\omega) = -\frac{4}{m\epsilon_0 E_0^2}\frac{d^2 f_0(0)}{dv^2}\int_{\min(-e\phi)}^{+\infty} dW\, \frac{1}{\bar{v}'}(W\bar{v}' - \frac{\bar{v}}{2})^2. \quad (1.68)$$

Assuming that the potential field $\phi(x)$ is still essentially sinusoidal, the average velocity $\bar{v}$ is given by Eqs. (A.5) and (A.7) for passing and trapped particles respectively. Furthermore, for passing particles one has $\langle H/v(x,W)\rangle_x = \tau_t/\lambda_0$ where τ_t is the transit time given by relation (A.4), while for trapped particles $\langle H/v(x,W)\rangle_x = \tau_b/(2\lambda_0)$, where τ_b is the bounce period given by (A.6). In terms of the energy variable κ, defined in Eq.(A.3), these terms thus read for passing particles ($0 < \kappa < 1$):

$$\begin{aligned}
\bar{v} &= \frac{2}{\pi}\frac{\Delta v_{\mathrm{trap}}}{\kappa}E(\kappa^2), \\
\bar{v}' &= \frac{2}{\pi}\frac{\kappa F(\kappa^2)}{m\Delta v_{\mathrm{trap}}},
\end{aligned}$$

and for trapped particles ($\kappa > 1$):

$$\begin{aligned}
\bar{v} &= \frac{2\Delta v_{\mathrm{trap}}}{\pi}\left[E(\frac{1}{\kappa^2}) + (\frac{1}{\kappa^2} - 1)F(\frac{1}{\kappa^2})\right], \\
\bar{v}' &= \frac{2}{\pi}\frac{F(\frac{1}{\kappa^2})}{m\Delta v_{\mathrm{trap}}}.
\end{aligned}$$

By inserting these last relations into Eq. (1.68), one then finally obtains:

$$
\begin{aligned}
\epsilon_L(k_0,\omega) &= -\frac{1}{2\pi}\frac{m\Delta v_{\text{trap}}^5}{\epsilon_0\,E_0^2}\left.\frac{d^2 f_0}{dv^2}\right|_{v_\phi}\left\{\int_0^1 \frac{d\kappa}{\kappa^6}\frac{1}{F(\kappa^2)}\left[(2-\kappa^2)F(\kappa^2)-2E(\kappa^2)\right]^2\right.\\
&\qquad\left.+\int_1^\infty \frac{d\kappa}{\kappa^3}\frac{1}{F(\frac{1}{\kappa^2})}\left[F(\frac{1}{\kappa^2})-2E(\frac{1}{\kappa^2})\right]^2\right\},\\
&= -\frac{\omega_p^2}{k_0^2}\Delta v_{\text{trap}}\left.\frac{d^2(f_0/N)}{dv^2}\right|_{v_\phi}\frac{8}{\pi}\int_0^1 d\kappa\left\{\underbrace{\frac{1}{\kappa^6 F}\left[2(F-E)-\kappa^2F\right]^2}_{\text{passing}}+\underbrace{\frac{\kappa}{F}(F-2E)^2}_{\text{trapped}}\right\},
\end{aligned}
\tag{1.69}
$$

having used the shortened notations $F = F(\kappa^2)$ and $E = E(\kappa^2)$ for the final equality. To obtain (1.69) one has transformed integration variable W to κ, so that $W = (m\Delta v_{\text{trap}}^2/4)(2/\kappa^2-1)$ and $dW = (m\Delta v_{\text{trap}}^2/\kappa^3)d\kappa$. For the trapped particle contribution, one has furthermore carried out the transformation $\kappa \to 1/\kappa$. The integral $\alpha = (8/\pi)\int d\kappa\ldots$ in (1.69) is a constant, and can be integrated numerically, providing the value $\alpha = 0.823$, which is composed of the contribution $\alpha^{\text{u}} = 0.117$ from untrapped particles and $\alpha^{\text{t}} = 0.705$ from trapped particles.

For a mode with given wave number k_0, the non-linear correction derived in Eq.(1.69) to the linear dispersion relation $\epsilon_{\text{L}}(k_0,\omega_{\text{L}}) = 0$, obviously leads to a shift $\delta\omega$ of the linear frequency ω_{L}. By assuming the non-linear effect small, so that one may expand $\epsilon_{\text{L}}(\omega_{\text{L}}+\delta\omega) = \epsilon_{\text{L}}(\omega_{\text{L}}) + \delta\omega\,\partial\epsilon_{\text{L}}(\omega_{\text{L}})/\partial\omega + \ldots \simeq \delta\omega\,\partial\epsilon_{\text{L}}(\omega_{\text{L}})/\partial\omega$, one obtains:

$$
\delta\omega = -\frac{\alpha}{\frac{\partial\epsilon_{\text{L}}(\omega_{\text{L}})}{\partial\omega}}\frac{\omega_p^2}{k_0^2}\Delta v_{\text{trap}}\left.\frac{d^2(f_0/N)}{dv^2}\right|_{v_\phi} = -\frac{\alpha}{2}\frac{\omega_p^3}{k_0^2}\Delta v_{\text{trap}}\left.\frac{d^2(f_0/N)}{dv^2}\right|_{v_\phi},
$$

having again made use of the cold fluid approximation $\epsilon_{\text{L}} \simeq 1-\omega_p^2/\omega^2$ for the dispersion function of electron plasma waves. This frequency shift is shown for Langmuir waves in Fig. 1.8 for both the initial value problem considered here (="sudden"), as well as for the case of a wave turned on adiabatically (="adiabatic". See exercise 1.2.6.1).

Exercises:

1.2.6.1 Derive the non-linear frequency shift in the case of a Langmuir wave turned on adiabatically instead of "suddenly", as in the initial value problem which has been considered in this section. Start by deriving the distribution $f^{\text{adiab.}}$ by invoking the invariance of the action $\int dxv$ as the amplitude of the wave is slowly turned on. This distribution is to be compared to the asymptotic distribution f_∞ considered in the initial value case. This exercise illustrates the non-uniqueness of the trapped particle distribution for a given wave amplitude, and thus reflects the potential diversity of BGK modes.

1.2.6.2 Adapt the derivation in this section to handle the non-linear frequency shift of an ion acoustic wave. Point out the contribution to the frequency shift from both the ions and the electrons.

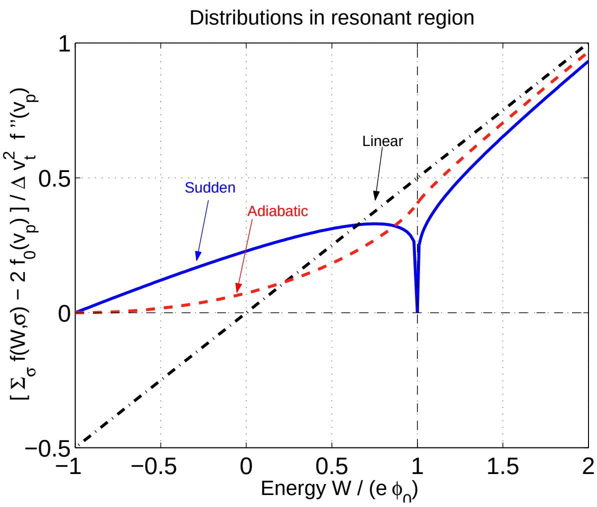

Figure 1.7: Distributions in resonant region for the linear, "sudden", and "adiabatic" cases. For the non-linear distributions, a sinusoidal wave is assumed. The "sudden" distribution corresponds to the initial value case considered in the main text, while the "adiabatic" case corresponds to the distribution obtained by adiabatically turning on the wave, and is addressed in exercise 1.2.6.1.

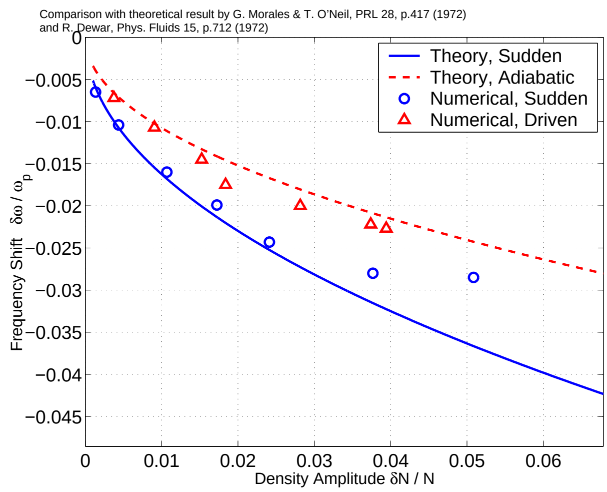

Figure 1.8: Non-linear frequency shift of a Langmuir wave as a function of the density perturbation amplitude $\delta N/N$. The considered wave number is $k_0\lambda_D = 1/3$. The numerical simulation results from the SAPRISTI code are compared to the analytic predictions for both the "sudden" and "adiabatic" case.

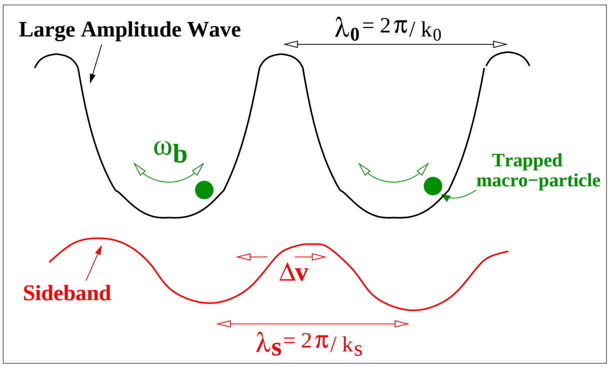

Figure 1.9: Resonant interaction of trapped particles with sidebands.

1.2.7 Stability of BGK Mode: The Trapped Particle Instability

In general, the undamped BGK modes are not stable equilibrium states. Indeed, they are subject to be destabilized by the growth of sidebands, which may be resonantly driven by the particles trapped in the principal wave. The resonant mechanism of this trapped particle instability (also called modulational instability) is schematized in Fig. 1.9.

1.2.8 Further Reading

- **Non-linear Landau damping and frequency shift:** See O'Neil [6], Morales and O'Neil [8], and Dewar [9].
- **BGK waves:** Bernstein, Greene, and Kruskal [7].
- **Trapped Particle Instability:** Kruer *et. al* [10], Goldman [11], and Dewar *et. al* [12].
- **Experimental evidence of non-linear evolution:** Danielson *et. al* [3] and the references therein.

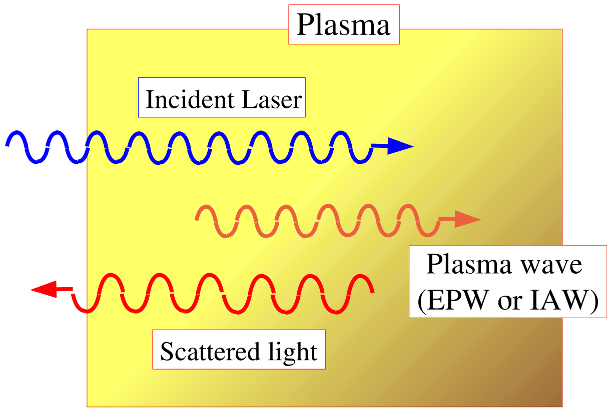

Figure 1.10: Basic mechanism of a parametric instability that may affect a laser beam in a plasma: The incident light (= wave #1), scatters off a plasma wave (= wave # 2), i.e. either an electron plasma wave (EPW) or an ion acoustic wave (IAW). If the matching conditions are met, the scattered light (= wave # 3) and the incident light may beat together in such a way as to reinforce the plasma wave.

1.3 Three Wave Interactions and Parametric Instabilities

Parametric instabilities result from the resonant interaction between three non-linearly coupled waves. The basic mechanism is schematized in figure 1.10 in the case of a laser beam, i.e. a transverse electromagnetic wave, propagating through an unmagnetized, under-dense plasma (frequency ω_0 of incident light $>$ plasma frequency ω_p). This incident light will reflect off any electron density fluctuation, in particular perturbations related to electron plasma waves (EPWs) or ion acoustic waves (IAWs). Under conditions of appropriate phase matching, the scattered and incident light may beat together in such a way as to reinforce the plasma wave (= EPW or IAW) via the ponderomotive force drive. This reinforced plasma wave will in turn lead to a higher level of scattering, and this increased scattered light will lead to a stronger beating with the incident light, which will increase the drive of the plasma wave, thus accelerating its amplification, obviously initiating an instability. The case of an electromagnetic wave scattering off an EPW is called Stimulated Raman Scattering (SRS), while the case of an electromagnetic wave scattering off an IAW is called Stimulated Brillouin Scattering (SBS).

The cases of SRS and SBS, as parametric instabilities affecting laser light propagating through a plasma, are of particular concern in the context of inertial fusion, as they lead to a loss of control of the laser energy deposition. Due to the relative simplicity in modeling these particular parametric instabilities (mainly the fact that they involve waves in a non-magnetized plasma), they will also be considered as illustrations in the following. However, it is important to emphasize the generality of the underlying instability mechanism which may affect any set of three non-linearly coupled waves verifying the appropriate matching conditions.

1.3.1 System of Three Coupled Oscillators

The problem of three non-linearly interacting waves is closely related to the dynamics of a system of three coupled oscillators. One therefore starts by considering this somewhat simpler system. This exercise will in particular point out the necessary condition of phase matching in time.

A system of three non-linearly coupled oscillators can be characterized by a Hamiltonian of the form:

$$H(x,p) = \sum_{j=1}^{3} \left(\frac{p_j^2}{2} + \omega_j^2 \frac{x_j^2}{2} \right) + V x_1 x_2 x_3, \tag{1.70}$$

where x_j, p_j, and ω_j are respectively the position, momentum, and eigenfrequency of the jth oscillator. The strength of the non-linear coupling is defined by the constant $V \in \mathbb{R}_+$.

The Hamilton-Jacobi equations:

$$\frac{dx_j}{dt} = \frac{\partial H}{\partial p_j}, \qquad\qquad \frac{dp_j}{dt} = -\frac{\partial H}{\partial x_j},$$

lead in the case of H given by (1.70) to the following set of coupled equations:

$$\ddot{x}_1 + \omega_1^2 x_1 = -V x_2 x_3, \tag{1.71}$$
$$\ddot{x}_2 + \omega_2^2 x_2 = -V x_1 x_3, \tag{1.72}$$
$$\ddot{x}_3 + \omega_3^2 x_3 = -V x_1 x_2. \tag{1.73}$$

The left hand sides of these equations clearly correspond to the linear equation of motion for each independent harmonic oscillator, while the right hand sides model a quadratic non-linear coupling. The doted quantities correspond to the standard notation for time differentiation.

If the non-linear coupling remains relatively small ($|V x_j| \ll |\omega_{j'}^2|$), a logical representation for the solution to the system (1.71)-(1.73) is of the form:

$$x_j(t) = \frac{1}{2} \left[A_j(t) e^{i\omega_j t} + A_j^\star(t) e^{-i\omega_j t} \right], \tag{1.74}$$

where the (possibly complex) amplitude $A_j(t)$ of the j'th oscillator is expected to vary slowly compared to the frequency ω_j, i.e. $|(dA_j/dt)/A_j| \ll |\omega_j|$.

Note, that if one wants to make use of a complex representation, one must be somewhat more careful for the non-linear physical system considered here than in the case of a linear one. Indeed, if C is a complex solution to a linear, physical (implying with real coefficients) set of equations, then the real part $\mathrm{Re}(C)$ and imaginary part $\mathrm{Im}(C)$ are obviously solutions as well. This property is not verified in the case of a non-linear system as a result of $\mathrm{Re}(z_1 z_2)$ which in general is not equal to $\mathrm{Re}(z_1)\mathrm{Re}(z_2)$, where $z_{1,2}$

are complex values. When dealing with a non-linear physical system, one must therefore ensure reality of the solutions from the start, which explains the presence of the complex conjugate term in Eq. (1.74).

Differentiating relation (1.74) with respect to time leads to

$$\begin{aligned}\dot{x}_j(t) &= \frac{1}{2}\left[(\dot{A}_j + i\omega_j A_j)e^{i\omega_j t} + \text{c.c.}\right], &(1.75)\\ \ddot{x}_j(t) &= \frac{1}{2}\left[(\ddot{A}_j + 2i\omega_j \dot{A}_j - \omega_j^2 A_j)e^{i\omega_j t} + \text{c.c.}\right]\\ &= \frac{1}{2}\left[(\ddot{A}_j + 2i\omega_j \dot{A}_j)e^{i\omega_j t} + \text{c.c.}\right] - \omega_j^2 x_j, &(1.76)\end{aligned}$$

where "c.c." stands for complex conjugate. Inserting (1.76) into (1.71) provides an equation for oscillator #1:

$$(\ddot{A}_1 + 2i\omega_1 \dot{A}_1)e^{i\omega_1 t} + \text{c.c.} = -\frac{V}{2}\left[A_2 A_3 e^{i(\omega_2+\omega_3)t} + A_2 A_3^\star e^{i(\omega_2-\omega_3)t} + \text{c.c.}\right],$$

which, after multiplying by $\exp(-i\omega_1 t)$, becomes:

$$\begin{aligned}(\ddot{A}_1 + 2i\omega_1 \dot{A}_1) + (\ddot{A}_1^\star - 2i\omega_1 \dot{A}_1^\star)e^{-2i\omega_1 t} &= -\frac{V}{2}\left[A_2 A_3 e^{-i(\omega_1-\omega_2-\omega_3)t} + A_2 A_3^\star e^{-i(\omega_1-\omega_2+\omega_3)t}\right.\\ &\quad \left. + A_2^\star A_3 e^{-i(\omega_1+\omega_2-\omega_3)t} + A_2^\star A_3^\star e^{-i(\omega_1+\omega_2+\omega_3)t}\right].(1.77)\end{aligned}$$

To obtain a slow time scale equation for the amplitude $A_1(t)$, one averages this last relation over the fast time scale of the eigenfrequencies ω_j. Note, that the assumption of time scale separation $|\dot{A}_j/A_j| \ll |\omega_j|$ also enables to neglect the terms $\ddot{A}_j$ compared to $2i\omega_j \dot{A}_j$ on the right hand side of Eq.(1.77).

In the case of frequency mismatch, such that all the phase factors $\exp -i(\omega_1 \pm \omega_2 \pm \omega_3)t$ on the right hand side of Eq.(1.77) vary on the fast time scale, i.e.

$$|\omega_1 \pm \omega_2 \pm \omega_3| \sim |\omega_j|,$$

the averaging process applied to Eq.(1.77) simply leads to

$$2i\omega_1 \dot{A}_1 = 0 \qquad \Longrightarrow \qquad A_1 = \text{const.},$$

Equivalent equations for A_2 and A_3 are also obtained by starting from Eqs. (1.72) and (1.73) respectively. This result clearly shows that in the case of frequency mismatch the oscillators are essentially decoupled, so that in the absence of damping their amplitude remains constant.

However, if the condition of resonant coupling is verified, i.e.

$$\omega_1 = \omega_2 + \omega_3 + \delta\omega, \tag{1.78}$$

the fast time scale averaging of Eq. (1.77) gives:

$$2i\omega_1\dot{A}_1 = -\frac{V}{2}A_2A_3e^{-i\,\delta\omega\,t}.$$

In Eq. (1.78) one has nonetheless allowed for the possibility of a small mismatch $\delta\omega$, but this mismatch is assumed small such that $|\delta\omega| \ll |\omega_j|$. Similar equations for A_2 and A_3 are obtained from Eqs. (1.72)-(1.73), providing the following system of non-linearly coupled equations for the slow time scale variation of the oscillator amplitudes A_j:

$$\begin{aligned} 2i\omega_1\dot{A}_1 &= -\frac{V}{2}A_2A_3e^{-i\,\delta\omega\,t}, && (1.79)\\ 2i\omega_2\dot{A}_2 &= -\frac{V}{2}A_1A_3^\star e^{+i\,\delta\omega\,t}, && (1.80)\\ 2i\omega_3\dot{A}_3 &= -\frac{V}{2}A_1A_2^\star e^{+i\,\delta\omega\,t}. && (1.81)\end{aligned}$$

From the set of equations (1.79)-(1.81) one can now start by carrying out a stability analysis of the state of the system in which one assumes that the oscillator #1 has been initially excited with a much larger amplitude than the two other ones. Thus, considering A_2 and A_3 as small perturbations compared to A_1 ($|A_{2,3}| \ll |A_1|$), one can linearize the system (1.79)-(1.81), which leads to

$$\begin{aligned} 2i\omega_1\dot{A}_1 &= 0 \qquad \Longrightarrow \qquad A_1 = A_{1,0} = \text{const},\\ 2i\omega_2\dot{A}_2 &= -\frac{V}{2}A_{1,0}A_3^\star e^{+i\,\delta\omega\,t},\\ 2i\omega_3\dot{A}_3 &= -\frac{V}{2}A_{1,0}A_2^\star e^{+i\,\delta\omega\,t}.\end{aligned}$$

By considering the Ansatz $A_2(t) = a_2\exp[(\gamma+i\,\delta\omega/2)t]$ and $A_3(t) = a_3\exp[(\gamma^\star+i\,\delta\omega/2)t]$, one then obtains:

$$\left\{\begin{aligned} 2i\omega_2(\gamma+i\tfrac{\delta\omega}{2})\,a_2 &= -\tfrac{V}{2}A_{1,0}\,a_3^\star,\\ 2i\omega_3(\gamma^\star+i\tfrac{\delta\omega}{2})\,a_3 &= -\tfrac{V}{2}A_{1,0}\,a_2^\star,\end{aligned}\right. \quad\Longleftrightarrow\quad \begin{pmatrix} 2i\omega_2(\gamma+i\frac{\delta\omega}{2}) & \frac{V}{2}A_{1,0}\\ \frac{V}{2}A_{1,0}^\star & -2i\omega_3(\gamma-i\frac{\delta\omega}{2})\end{pmatrix}\begin{pmatrix} a_2\\ a_3^\star\end{pmatrix} = \begin{pmatrix}0\\0\end{pmatrix}$$

To obtain a solution with non-zero amplitudes $a_{2,3}$, the determinant of this last linear system must be zero, which provides the following relation for γ:

$$\gamma^2 = \left(\frac{V}{4}\right)^2\frac{|A_{1,0}|^2}{\omega_2\omega_3} - \left(\frac{\delta\omega}{2}\right)^2. \tag{1.82}$$

To have instability requires $\gamma^2 > 0$. From Eq. (1.82), a necessary condition for instability is thus

$$\omega_2\,\omega_3 > 0, \tag{1.83}$$

which is also a sufficient condition if there is no mismatch ($\delta\omega = 0$). The two conditions (1.78) and (1.83) thus lead to

$$|\omega_1| > |\omega_2|, |\omega_3|.$$

Here the conditions for instability must be interpreted as the conditions for effective energy transfer from oscillator #1 to the oscillators #2 and #3. We thus conclude that for this transfer to be effective, the frequency ω_1 of oscillator #1 must be larger than the frequencies of the other two oscillators. In the frame of a quantum description, equations (1.78) and (1.83) correspond to the energy conservation for one quantum of oscillator #1 decaying into one quantum of oscillator # 2 and one quantum of oscillator #3:

$$\hbar|\omega_1| = \hbar|\omega_2| + \hbar|\omega_3|.$$

In the presence of a frequency mismatch, condition (1.83) is obviously not sufficient for instability. From Eq. (1.82), one clearly sees that there is an additional condition on the amplitude of oscillator #1:

$$|A_{1,0}| > \frac{2|\delta\omega|(\omega_2\omega_3)^{1/2}}{V}.$$

Exercises:

1.3.1.1 Re-derive the system of equations (1.79)-(1.81) but furthermore assuming that the j'th oscillator undergoes damping with rate γ_j. Repeat the linear stability analysis against parametric instabilities (for this, neglect the damping of oscillator #1), and show that the relation (1.82) for the rate γ now becomes:

$$\gamma = -\frac{\gamma_2+\gamma_3}{4} \pm \left[\left(\frac{\gamma_2-\gamma_3}{4} + i\frac{\delta\omega}{2}\right)^2 + \left(\frac{V}{4}\right)^2 \frac{|A_{1,0}|^2}{\omega_2\omega_3}\right]^{1/2}$$

Re-assess the conditions for instability in this case. In particular, show that there is now an amplitude threshold even in the case of perfect frequency match ($\delta\omega = 0$).

1.3.2 Illustration of Three Wave Coupling: Stimulated Raman Scattering

As has been done in the previous section for the amplitudes of three coupled harmonic oscillators, one now derives the equations governing the evolution of the envelopes of three non-linearly interacting waves. This derivation is carried out here for the particular case of stimulated Raman scattering (SRS), which, as we recall, involves the interaction of

1. An incident electromagnetic wave, the so-called pump.
2. A scattered electromagnetic wave.
3. An electron plasma wave (EPW).

The specific case of SRS enables to illustrate the derivation of a system of coupled equations for the wave amplitudes whose form is generic for any set of three non-linearly interacting waves.

SRS involves two types of waves: Transverse electromagnetic waves, and electron plasma

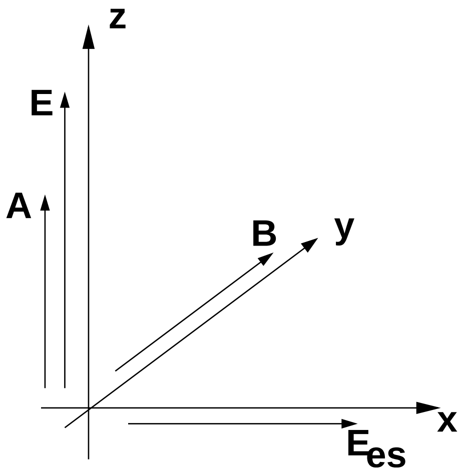

Figure 1.11: Fields ($\vec{E} = E_z\vec{e}_z$, $\vec{B} = B_y\vec{e}_y$) of linearly polarized electromagnetic waves represented by the vector potential $\vec{A} = A_z\vec{e}_z$ and electrostatic field $\vec{E}_{\rm es} = E_x\vec{e}_x$ of plasma wave, for slab model of SRS and SBS.

waves. One thus needs to derive the corresponding wave equations, and in particular identify the dominant non-linear coupling terms. As the coupling involves no essential wave-particle resonance, these equations are derived, for simplicity, in the frame of a fluid description. One assumes furthermore the system to be one-dimensional (slab), so that all fields depend on a single spatial variable x.

Equation for Transverse EM Waves

One starts by deriving the wave equation for the transverse EM waves. The corresponding electric and magnetic fields ($\vec{E}, \vec{B}$) verify Maxwell's equations, and in particular

$$\begin{aligned} \nabla \times \vec{E} &= -\frac{\partial \vec{B}}{\partial t}, \\ \nabla \cdot \vec{B} &= 0. \end{aligned}$$

The general solution to these two equations can be expressed in terms of the vector potential $\vec{A}$ and scalar potential ϕ:

$$\vec{E} = -\frac{\partial \vec{A}}{\partial t} - \nabla\phi, \qquad \vec{B} = \nabla \times \vec{A}.$$

In Coulomb gauge, for which $\nabla \cdot \vec{A} = 0$, one has for a transverse wave

$$\nabla \cdot \vec{E} = -\triangle\,\phi = 0 \qquad \Longrightarrow \qquad \phi = 0.$$

One shall furthermore assume here that the transverse wave is linearly polarized along the direction Oz (see Fig. 1.11), so that $\vec{A} = A_z(x,t)\,\vec{e}_z$, and

$$\vec{E} = E_z\,\vec{e}_z = -\frac{\partial A_z}{\partial t}\,\vec{e}_z, \qquad \vec{B} = B_y\,\vec{e}_y = -\frac{\partial A_z}{\partial x}\,\vec{e}_y. \tag{1.84}$$

Inserting these relations into Ampere's law

$$\nabla \times \vec{B} = \mu_0 \vec{j} + \frac{1}{c^2}\frac{\partial \vec{E}}{\partial t},$$

provides

$$\frac{1}{c^2}\frac{\partial^2 A_z}{\partial t^2} = \frac{\partial^2 A_z}{\partial x^2} + \mu_0 j_z, \tag{1.85}$$

where c is the speed of light, and j_z is the current along $\vec{e}_z$ induced by the EM fields in the plasma. This plasma current is derived from the equation of motion for the particles:

$$m\frac{d\vec{v}}{dt} = q\,(\vec{E} + \vec{v} \times \vec{B}).$$

Projecting onto $\vec{e}_z$ and inserting relations (1.84) provides:

$$m\frac{dv_z}{dt} = q\,(E_z + v_x B_y) = -q\,(\frac{\partial A_z}{\partial t} + v_x\frac{\partial A_z}{\partial x}) = -q\frac{dA_z}{dt} \qquad \Longrightarrow \qquad \frac{d}{dt}(mv_z + qA_z) = 0.$$

This last relation expresses the invariance of momentum $\vec{p} = m\vec{v} + q\vec{A}$ along Oz, which results from the fact that the system is translationally invariant in this direction. If the particles are essentially immobile before the passage of the wave, one obtains

$$v_z = -\frac{qA_z}{m}, \tag{1.86}$$

so that the transverse current can be written

$$j_z = \sum_{\text{species}} Nqv_z = -A_z \sum_{\text{species}} \frac{Nq^2}{m} \simeq -\frac{N_e e^2}{m_e} A_z, \tag{1.87}$$

having only kept the electron contribution, as the ion contribution is smaller by the ratio m_e/m_i. To lighten notations, the subscript "e" for electron values will be dropped from here on.

By considering the electron density $N = N_0 + \delta N$ as the superposition of an initial, homogeneous background N_0 and of fluctuations δN, one finally obtains by inserting (1.87) in (1.85):

$$\frac{\partial^2 A_z}{\partial t^2} - c^2\frac{\partial^2 A_z}{\partial x^2} + \omega_p^2 A_z = -\omega_p^2 \frac{\delta N}{N_0} A_z, \tag{1.88}$$

where $\omega_p^2 = N_0\, e^2/m\epsilon_0$ is the plasma frequency squared. The left hand side of this last equation is simply the linear wave equation for transverse electromagnetic waves, giving rise to the dispersion relation $\omega^2 = \omega_p^2 + (kc)^2$, and in particular to the well-known condition for propagation $|\omega| > \omega_p$. Longitudinal plasma waves (either EPWs or IAWs) are naturally a source of density fluctuations δN, so that the term on the right hand side of Eq. (1.88) provides the non-linear coupling term between the transverse EM waves and the plasma waves.

Equation for Electron Plasma Waves

For modeling the high frequency EPWs, one can treat the massive ions as an immobile, uniform, neutralizing background. The electrons are modeled here with a warm fluid description. For this, one considers the continuity equation and momentum equation along Ox:

$$\begin{aligned} \frac{\partial N}{\partial t} + \frac{\partial}{\partial x}(N v_x) &= 0, &(1.89)\\ mN\,(\frac{\partial v_x}{\partial t} + v_x \frac{\partial v_x}{\partial x}) &= -eN\,(E_x - v_z B_y) - \frac{\partial p}{\partial x}, &(1.90) \end{aligned}$$

as well as the closure from the equation of state:

$$\frac{p}{N^\gamma} = \text{const.}, \tag{1.91}$$

where p is the electronic pressure. For EPWs, the phase velocity $v_\phi = \omega/k$ is such that $|v_\phi| \gg v_{\text{th}}$. One thus considers the adiabatic equation of state for which $\gamma = (D+2)/D$, where D is the number of degrees of freedom. For wave propagation the appropriate value is $D = 1$, so that $\gamma = 3$.

The electric component E_x on the right hand side of Eq. (1.90) corresponds to the longitudinal, electrostatic field related to the EPWs, and verifies Poisson's equation:

$$\frac{\partial E_x}{\partial x} = -\frac{e\,\delta N}{\epsilon_0}. \tag{1.92}$$

where δN is the electron density perturbation related to the EPWs.

The next term on the right hand side of Eq. (1.90) is the Lorentz force $F_p = e\,v_z B_y$, which results from the transverse oscillatory motion represented by Eq. (1.86), and gives rise to the so-called ponderomotive force:

$$F_p = e\,v_z B_y = e\,\frac{eA_z}{m}(-\frac{\partial A_z}{\partial x}) = -\frac{1}{2}\frac{\partial}{\partial x}(\frac{e^2 A_z^2}{m}).$$

The ponderomotive force provides the non-linear coupling of the EPWs with the transverse EM waves. This is therefore the only non-linearity which is retained, and all other terms in Eqs. (1.89)-(1.91) are linearized with respect to the EPW perturbation terms δN, v_x, E_x and δp:

$$\frac{\partial\,\delta N}{\partial t} + N_0 \frac{\partial\,v_x}{\partial x} = 0, \tag{1.93}$$

$$\begin{aligned} m\,\frac{\partial\,v_x}{\partial t} &= -e\,E_x - \frac{1}{2}\frac{\partial}{\partial x}(\frac{e^2 A_z^2}{m}) - \frac{1}{N_0}\frac{\partial \delta p}{\partial x}, &(1.94)\\ \delta p &= \gamma\,\frac{p_0}{N_0}\delta N = 3\,T_0\,\delta N, &(1.95) \end{aligned}$$

having used $p_0 = N_0 T_0$, where T_0 is the background electron temperature.

Inserting Eq. (1.92) into Eqs. (1.93) and (1.95) enables to express the longitudinal velocity and pressure perturbations in terms of E_x:

$$\begin{aligned} v_x &= \frac{\epsilon_0}{e\,N_0}\frac{\partial E_x}{\partial t}, \\ \delta p &= -3\,\epsilon_0 \frac{T_0}{e}\frac{\partial E_x}{\partial x}. \end{aligned}$$

These relations are in turn inserted into Eq. (1.94), finally providing:

$$\frac{\partial^2 E_x}{\partial t^2} - 3v_{\mathrm{th}}^2 \frac{\partial^2 E_x}{\partial x^2} + \omega_p^2 E_x = -\omega_p^2 \frac{1}{2}\frac{\partial}{\partial x}\frac{eA_z^2}{m}. \tag{1.96}$$

The left hand side of Eq. (1.96) is clearly the linear wave equation for EPWs, leading to the Bohm-Gross dispersion relation $\omega^2 = \omega_p^2 + 3(kv_{\mathrm{th}})^2$. The right hand side represents the non-linear coupling with the transverse EM waves.

Coupled Three Wave Equations

To summarize the above results, one rewrites here the wave equations for the transverse EM waves with vector potential component A_z and EPWs with electrostatic component E_x:

$$\frac{\partial^2 A_z}{\partial t^2} - c^2 \frac{\partial^2 A_z}{\partial x^2} + \omega_p^2 A_z = \frac{e}{m}\frac{\partial E_x}{\partial x} A_z, \tag{1.97}$$

$$\frac{\partial^2 E_x}{\partial t^2} - 3v_{\mathrm{th}}^2 \frac{\partial^2 E_x}{\partial x^2} + \omega_p^2 E_x = -\omega_p^2 \frac{1}{2}\frac{\partial}{\partial x}\frac{eA_z^2}{m}, \tag{1.98}$$

having used (1.92) to replace δN by E_x in Eq. (1.88).

To obtain a model for SRS, one now intends to derive from Eqs. (1.97)–(1.98) a system of coupled equations for the amplitudes $\mathcal{A}_0$, $\mathcal{A}_s$ and $\mathcal{E}$ of the incident EM wave, scattered EM wave, and the EPW respectively. The method for deriving these equations is similar to the one used for obtaining the system (1.79)–(1.81) for the amplitudes of three coupled harmonic oscillators, with the additional complication however of spatial dependence.

Under the assumption of small non-linear coupling, it is logical to assume that each wave involved in the SRS mechanism has a wave number k and frequency ω still verifying the linear dispersion relation, but with an amplitude that may vary slowly both in space and time. The vector potential field A_z in Eqs. (1.97)–(1.98), which is the superposition of the incident and scattered EM waves, is thus written:

$$A_z(x,t) = \underbrace{\frac{1}{2}\left[\mathcal{A}_0(x,t)\, e^{i(k_0 x - \omega_0 t)} + \text{c.c.}\right]}_{\text{Incident EM}} + \underbrace{\frac{1}{2}\left[\mathcal{A}_s(x,t)\, e^{i(k_s x - \omega_s t)} + \text{c.c.}\right]}_{\text{Scattered EM}}, \tag{1.99}$$

while a similar Ansatz is considered for the electrostatic field:

$$E_x(x,t) = \underbrace{\frac{1}{2}\left[\mathcal{E}(x,t)\, e^{i(k_e x - \omega_e t)} + \text{c.c.}\right]}_{\text{EPW}}, \tag{1.100}$$

where the wave number-frequency pairs (k, ω) of all three waves verify their respective linear dispersion relations:

$$\omega_0^2 = \omega_p^2 + (k_0 c)^2, \tag{1.101}$$
$$\omega_s^2 = \omega_p^2 + (k_s c)^2, \tag{1.102}$$
$$\omega_e^2 = \omega_p^2 + 3(k_e v_{\text{th}})^2. \tag{1.103}$$

As an example, the condition of slowly varying envelopes reads in the case of the incident EM wave:

$$|\frac{1}{\mathcal{A}_0}\frac{\partial \mathcal{A}_0}{\partial x}| \ll |k_0|, \qquad \text{and} \qquad |\frac{1}{\mathcal{A}_0}\frac{\partial \mathcal{A}_0}{\partial t}| \ll |\omega_0|.$$

Similar scalings hold for $\mathcal{A}_s$ and $\mathcal{E}$.

To obtain the equations for the amplitudes $\mathcal{A}_0$ and $\mathcal{A}_s$ for the incident and scattered EM waves, one starts by differentiating Eq. (1.99) with respect to x and t:

$$\begin{aligned}
\partial_x A_z &= \sum_{0,s} \frac{1}{2}\left[(\partial_x \mathcal{A} + ik\mathcal{A})\, e^{i(kx-\omega t)} + \text{c.c.}\right], \\
\partial_{xx} A_z &= \sum_{0,s} \frac{1}{2}\left[(\partial_{xx} \mathcal{A} + 2ik\,\partial_x\mathcal{A} - k^2\mathcal{A})\, e^{i(kx-\omega t)} + \text{c.c.}\right], \\
\partial_t A_z &= \sum_{0,s} \frac{1}{2}\left[(\partial_t \mathcal{A} - i\omega\mathcal{A})\, e^{i(kx-\omega t)} + \text{c.c.}\right], \\
\partial_{tt} A_z &= \sum_{0,s} \frac{1}{2}\left[(\partial_{tt} \mathcal{A} - 2i\omega\,\partial_t\mathcal{A} - \omega^2\mathcal{A})\, e^{i(kx-\omega t)} + \text{c.c.}\right].
\end{aligned}$$

Differentiating Eq.(1.100) provides similar relations for E_x, which can then all be inserted into Eq.(1.97), leading to:

$$\begin{aligned}
&\frac{1}{2}\left[(\partial_{tt}\mathcal{A}_0 - 2i\omega_0\,\partial_t\mathcal{A}_0)\, e^{i(k_0x-\omega_0 t)} + \text{c.c.}\right] - c^2\frac{1}{2}\left[(\partial_{xx}\mathcal{A}_0 + 2ik_0\,\partial_x\mathcal{A}_0)\, e^{i(k_0x-\omega_0 t)} + \text{c.c.}\right] \\
&+\frac{1}{2}\left[(\partial_{tt}\mathcal{A}_s - 2i\omega_s\,\partial_t\mathcal{A}_s)\, e^{i(k_sx-\omega_s t)} + \text{c.c.}\right] - c^2\frac{1}{2}\left[(\partial_{xx}\mathcal{A}_s + 2ik_s\,\partial_x\mathcal{A}_s)\, e^{i(k_sx-\omega_s t)} + \text{c.c.}\right] \\
&\qquad = \frac{e}{m}\frac{1}{2}\left[(\partial_x\mathcal{E} + ik_e\,\mathcal{E})\, e^{i(k_ex-\omega_e t)} + \text{c.c.}\right] \times \\
&\qquad\qquad \left\{\frac{1}{2}\left[\mathcal{A}_0\, e^{i(k_0x-\omega_0 t)} + \text{c.c.}\right] + \frac{1}{2}\left[\mathcal{A}_s\, e^{i(k_sx-\omega_s t)} + \text{c.c.}\right]\right\}
\end{aligned} \tag{1.104}$$

having made use of Eqs. (1.101)-(1.102). Invoking the assumption of slow variation of the envelope, one has $|\partial_{tt}\mathcal{A}| \ll |\omega\,\partial_t\mathcal{A}|$, $|\partial_{xx}\mathcal{A}| \ll |k\,\partial_x\mathcal{A}|$ and $|\partial_x\mathcal{E}| \ll |k_e\,\mathcal{E}|$, which justifies neglecting these smaller terms in Eq.(1.104).

By multiplying Eq. (1.104) by $\exp -i(k_0 x - \omega_0 t)$ and averaging over the fast space and time scales of the wave numbers k and wave frequencies ω, one obtains a slow variation scale equation for the incident wave amplitude $A_0(x,t)$. Similarly as for the system of coupled harmonic oscillators, one sees that the non-linear coupling terms on the right hand side of Eq. (1.104) will in general average out to zero unless certain resonant conditions are met. These conditions correspond to phase matching of the three waves both in space and time, and can be written in terms of the wave numbers and frequencies as:

$$
\begin{aligned}
k_0 &= k_s + k_e, && (1.105)\\
\omega_0 &= \omega_s + \omega_e + \delta\omega, && (1.106)
\end{aligned}
$$

having allowed in (1.106) for a possible frequency mismatch $\delta\omega$, such that $|\delta\omega| \ll |\omega_{0,s,e}|$. Under these matching conditions, one then obtains after averaging:

$$
-2i\omega_0\, \partial_t \mathcal{A}_0 - c^2\, 2ik_0\, \partial_x \mathcal{A}_0 = \frac{e}{2m} ik_e\, \mathcal{E} \mathcal{A}_s\, e^{i\delta\omega t}.
$$

In the same way, by multiplying Eq. (1.104) by $\exp -i(k_s x - \omega_s t)$ and performing the same averaging leads to the corresponding equation for the scattered wave amplitude $A_s(x,t)$:

$$
-2i\omega_s\, \partial_t \mathcal{A}_s - c^2\, 2ik_s\, \partial_x \mathcal{A}_s = -\frac{e}{2m} ik_e\, \mathcal{E}^\star \mathcal{A}_0\, e^{-i\delta\omega t}.
$$

The equation for the EPW envelope $\mathcal{E}(x,t)$ is obtained through a similar derivation by inserting (1.99) and (1.100) into (1.98), multiplying by $\exp -i(k_e x - \omega_e t)$, and averaging. Again invoking the assumption of phase matching, one then obtains (check it as an exercise):

$$
-2i\omega_e\, \partial_t \mathcal{E} - 3v_{\mathrm{th}}^2\, 2ik_e\, \partial_x \mathcal{E} = -\frac{e}{2m} \omega_p^2\, ik_e\, \mathcal{A}_0 \mathcal{A}_s^\star\, e^{-i\delta\omega t}.
$$

The system of non-linearly coupled equations for the three wave amplitudes can thus be summarized as follows:

$$
\begin{aligned}
\partial_t \mathcal{A}_0 + v_{\mathrm{g},0}\, \partial_x \mathcal{A}_0 &= -\frac{e}{4m} \frac{k_e}{\omega_0}\ \ \mathcal{E}\, \mathcal{A}_s\, e^{i\delta\omega t}, && (1.107)\\
\partial_t \mathcal{A}_s + v_{\mathrm{g,s}}\, \partial_x \mathcal{A}_s &= \frac{e}{4m} \frac{k_e}{\omega_s}\ \ \mathcal{A}_0\, \mathcal{E}^\star\, e^{-i\delta\omega t}, && (1.108)\\
\partial_t \mathcal{E} + v_{\mathrm{g,e}}\, \partial_x \mathcal{E} &= \frac{e}{4m} \frac{k_e}{\omega_e} \omega_p^2\, \mathcal{A}_0\, \mathcal{A}_s^\star\, e^{-i\delta\omega t}, && (1.109)
\end{aligned}
$$

having used the notations $v_{\mathrm{g,0,s}} = d\omega_{0,s}/dk_{0,s} = c^2 k_{0,s}/\omega_{0,s}$ and $v_{\mathrm{g,e}} = d\omega_e/dk_e = 3v_{\mathrm{th}}^2 k_e/\omega_e$ for the group velocities of the three waves.

In case the phase matching conditions (1.105)–(1.106) are not verified, the non-linear coupling terms on the right hand sides of Eqs. (1.107)–(1.109) are absent. The resulting equations then simply represent the independent advection of the three wave envelopes at their respective group velocity. For example, for the incident wave:

$$\partial_t \mathcal{A}_0 + v_{\mathrm{g},0}\,\partial_x \mathcal{A}_0 = 0 \qquad \Longrightarrow \qquad \mathcal{A}_0(x,t) = \mathcal{A}_0(x - v_{\mathrm{g},0}\,t, t=0). \tag{1.110}$$

In the case of space independent wave amplitudes, one can easily show the equivalence of the system of coupled equations (1.107)-(1.109) with the system (1.79)-(1.81) for the amplitudes of the coupled harmonic oscillators. For this, one simply needs to identify the corresponding terms (harmonic oscillators $\leftrightarrow$ waves): $(A_1,\omega_1) \leftrightarrow (-i\mathcal{A}_0, -\omega_0)$, $(A_2,\omega_2) \leftrightarrow (-i\mathcal{A}_s, -\omega_s)$, $(A_3,\omega_3) \leftrightarrow (-i\mathcal{E}/\omega_p, -\omega_e)$, $V \leftrightarrow e\,k_e\,\omega_p/m$, and $\delta\omega \leftrightarrow -\delta\omega$.

Linear Analysis of the Parametric Instability

As in section 1.3.1, one can now start by carrying out a linear stability analysis of the state of the system in which the incident EM wave has an amplitude $\mathcal{A}_0$ significantly larger than the amplitudes $\mathcal{A}_s$ and $\mathcal{E}$ of the scattered wave and EPW respectively. In a real physical system, $\mathcal{A}_0$ could represent a high intensity laser beam, while the initial values of $\mathcal{A}_s$ and $\mathcal{E}$ could be at the level of thermal fluctuations. One furthermore assumes here that there is no spatial variations of the envelopes, so that only temporal variations are considered. Thus, considering $\mathcal{A}_s$ and $\mathcal{E}$ as small perturbations, one can linearize the system (1.107)-(1.109) with respect to these terms, which leads to

$$\begin{aligned}
\partial_t \mathcal{A}_0 &= 0 \qquad \Longrightarrow \qquad \mathcal{A}_0 = \text{const}, & (1.111)\\
\partial_t \mathcal{A}_s &= \frac{e}{4m}\frac{k_e}{\omega_s}\quad \mathcal{A}_0\,\mathcal{E}^\star\,e^{-i\delta\omega t}, & (1.112)\\
\partial_t \mathcal{E} &= \frac{e}{4m}\frac{k_e}{\omega_e}\,\omega_p^2\,\mathcal{A}_0\,\mathcal{A}_s^\star\,e^{-i\delta\omega t}. & (1.113)
\end{aligned}$$

Thus, considering $\mathcal{A}_0$ as a constant, Eqs. (1.112)-(1.113) become linear in $\mathcal{A}_s$ and $\mathcal{E}$. Solutions for these two fields can be found of the form $\mathcal{A}_s \sim \exp(\gamma - i\delta\omega/2)t$ and $\mathcal{E} \sim \exp(\gamma^\star - i\delta\omega/2)t$, which leads to the rate:

$$\gamma^2 = \left(\frac{k_e v_{\mathrm{os}}}{4}\right)^2 \frac{\omega_p^2}{\omega_s\omega_e} - \left(\frac{\delta\omega}{2}\right)^2, \tag{1.114}$$

where one has defined $v_{\mathrm{os}} = e|\mathcal{A}_0|/m$ the velocity oscillation amplitude of electrons in the incident EM wave. Note again the analogy between (1.114) and (1.82).

From Eq. (1.114), one sees that a necessary condition for instability is thus again $\omega_s\omega_e > 0$, which together with (1.106) implies that all three frequencies $\omega_{0,s,e}$ must have same sign, and that $|\omega_0| > |\omega_s|, |\omega_e|$. From here on, as a convention, all three frequencies $\omega_{0,s,e}$ can thus be assumed positive.

Exercises:

1.3.2.1 Carry out the derivation of equation (1.109).

1.3.2.2 How do Eqs. (1.107)-(1.109) generalize in the presence of possible damping mechanisms for the various waves?

1.3.2.3 Derive the non-linear coupling equations for the envelopes of the three waves involved in stimulated Brillouin scattering (SBS). Compute the corresponding linear growth rate of the parametric instability.

1.3.3 Matching Conditions

Let us make some additional comments here relative to the matching conditions for non-linear three wave coupling. For illustration purposes, one pursues this discussion in the particular case of SRS.

For the one-dimensional slab model of SRS that was considered in Sec. 1.3.2, it appears clearly, that having fixed one of the 6 real wave number-frequency values (k_0, ω_0), (k_s, ω_s) and (k_e, ω_e) the other values are in general determined by the system of 5 equations formed by the 3 dispersion relations (1.101)-(1.103) and the 2 matching conditions (1.105) and (1.106).

Note however, that the dispersion relations contain quadratic terms, and therefore, for a given incident wave with wave number-frequency pair (k_0, ω_0) their may be zero, one or two solutions for (k_s, ω_s) and (k_e, ω_e) verifying the matching conditions. Obviously, for SRS, as a result of the properties $\omega_s > \omega_p$ and $\omega_e > \omega_p$, one must have from (1.106) $\omega_0 > 2\omega_p$. By defining the critical density N_c such that $\omega_0^2 = N_c e^2/m\epsilon_0 = (N_c/N)\omega_p^2$, one thus obtains a necessary condition for SRS to be able to develop (density below quarter critical):

$$N < \frac{N_c}{4}.$$

The geometrical solution to the matching conditions (1.105)-(1.106) in a one-dimensional system appears as a sum of vectors in the (k, ω) plane: $(k_0, \omega_0) = (k_s, \omega_s) + (k_e, \omega_e)$, where the three vectors $(k_{0,s,e}, \omega_{0,s,e})$ must lie on the curves of their respective dispersion relation. This is shown in the case of SRS in Fig. 1.12. From this figure, one clearly sees that for $\omega_0 \gtrsim 2\omega_p$ there are in general two solutions to the matching conditions for a given incident wave (k_0, ω_0). One solution is such that $k_0 k_s < 0$, and is called Backward SRS (BSRS), as it corresponds to the scattered EM wave propagating opposite to the incident wave. The other solution with $k_0 k_s > 0$ is called Forward SRS (FSRS), and corresponds to the scattered wave propagating in the same direction as the incident one. According to (1.114), the SRS growth rate related to backward scattering tends to be larger than for forward scattering, as $|k_e^{\mathrm{BSRS}}| > |k_e^{\mathrm{FSRS}}|$. This is indeed true as long as damping of the EPW is not important. However, as Landau damping increases with $k_e\lambda_D$, FSRS can become competitive when $k_e^{\mathrm{BSRS}}\lambda_D$ becomes large.

Given the frequency ω_0 of the incident laser light, the matching conditions for SRS can thus be solved together with the dispersion relations to obtain the wave number-frequency

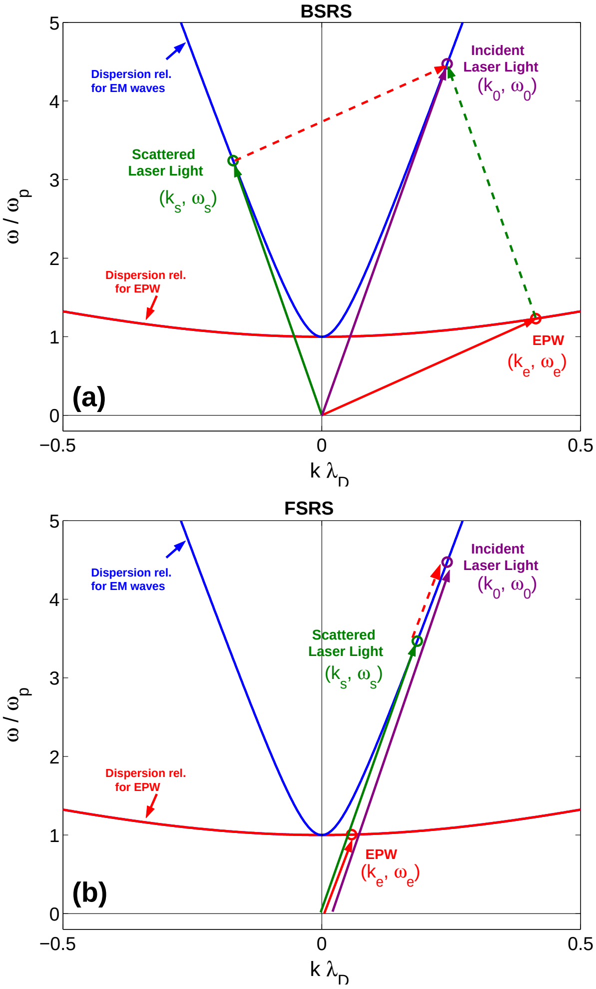

Figure 1.12: Geometrical solution to the matching conditions for (a) backward and (b) forward SRS. The blue curve corresponds to the dispersion relation $\omega^2 = \omega_p^2 + (kc)^2$ for electromagnetic waves, and the red curve shows the Bohm-Gross dispersion relation $\omega^2 = \omega_p^2 + 3(kv_{\text{th}})^2$ for EPWs. Space and time phase matching: The purple vector, representing the wave number and frequency (ω_0, k_0) of the incident laser light, must be the sum of the vectors (k_s, ω_s) and (k_e, ω_e) representing the scattered light and EPW respectively.

pairs of all waves involved in the SRS mechanism. This is achieved by first inserting (1.105) and (1.106) into (1.102), which (neglecting possible mismatch $\delta\omega$) leads to:

$$(\omega_0 - \omega_e)^2 = \omega_p^2 + (k_0 - k_e)^2 c^2.$$

Making use of Eq. (1.101) for (k_0, ω_0), this relation can then be reduced to

$$k_e^2 - 2k_0 k_e - \frac{\omega_e(\omega_e - 2\omega_0)}{c^2} = 0,$$

which in turn is solved for k_e:

$$\begin{aligned} k_e &= k_0 \pm \frac{1}{c}\,(k_0^2 c^2 + \omega_e^2 - 2\omega_0\omega_e)^{1/2} \\ &\simeq k_0 \pm \frac{\omega_0}{c}\,(1 - 2\frac{\omega_p}{\omega_0})^{1/2}, \end{aligned} \tag{1.115}$$

having approximated $\omega_e \simeq \omega_p$ in the last step, and having again invoked Eq. (1.101). From the matching condition on the wave numbers, one has $k_s = k_0 - k_e$, so that

$$k_s = \mp\frac{\omega_0}{c}\,(1 - 2\frac{\omega_p}{\omega_0})^{1/2}.$$

For $k_0 > 0$, the solution k_e with the + sign in (1.115) is thus related to BSRS, while the solution with the − sign corresponds to FSRS. From Eq.(1.115) it also appears clearly that k_e^{BSRS} varies from $2k_0$ in the limit of low density ($N \ll N_c/4 \Leftrightarrow \omega_0 \gg 2\omega_p$), down to k_0 in the limit $N \simeq N_c/4 \Leftrightarrow \omega_0 \simeq 2\omega_p$.

If the waves are allowed to propagate in more than one dimension, the wave number matching condition (1.105) is replaced by the *vector* equation on the wave vectors:

$$\vec{k}_0 = \vec{k}_s + \vec{k}_e. \tag{1.116}$$

In this case, having fixed for instance the frequency ω_0 and direction $\vec{n}_0 = \vec{k}_0/k_0$ of the incident wave, there remain 9 parameters to be determined for the wave vectors and frequencies of the three waves involved in the parametric instability: k_0, $(\vec{k}_s, \omega_s)$, and $(\vec{k}_e, \omega_e)$. These 9 parameters must verify the system of 7 equations formed by the 3 dispersion relations (1.101)-(1.103) and the 4 matching conditions (1.106) and (1.116). Thus, there remain 2 degrees of freedom. These can be chosen as the scattering direction $\vec{n}_s = \vec{k}_s/k_s$. Therefore, in general, scattering can occur in all spatial directions. Note however that each scattering direction has its own growth rate and interaction length.

In the context of a quantum description, the matching condition (1.116) on the wave vectors and the matching condition (1.106) on the frequencies correspond respectively to the conservation of momentum and energy of an incident photon scattering off a plasmon:

$$\hbar\vec{k}_0 = \hbar\vec{k}_s + \hbar\vec{k}_e, \tag{1.117}$$

$$\hbar\omega_0 = \hbar\omega_s + \hbar\omega_e, \tag{1.118}$$

where $(\hbar\vec{k}_0, \hbar\omega_0)$, $(\hbar\vec{k}_s, \hbar\omega_s)$, and $(\hbar\vec{k}_e, \hbar\omega_e)$ are respectively the (momentum, energy) of the incident photon, scattered photon, and plasmon involved in the process.

Exercises:

1.3.3.1 Draw the geometrical solution to the matching conditions for SBS.

1.3.3.2 From the appropriate plot, convince yourself that matching conditions can be verified for the potential decay of an EPW into another EPW and an IAW. This parametric instability is the so-called Langmuir Decay Instability (LDI).

1.3.4 Manley-Rowe Relations

One can show that the non-linear system of coupled equations (1.107)–(1.109) for the amplitudes of the three waves involved in the parametric instability verifies certain conservation laws. These laws are conveniently derived after an appropriate normalization of the wave amplitudes.

Inspired by the equivalence between the matching conditions on the wave vectors/frequencies of the waves in the classical description and the conservation laws (1.117)-(1.118) of the corresponding quantum process, one defines for each wave the complex action amplitude a, such that the corresponding action density $n = |a^2| = a\, a^\star$ is related to the wave energy density E_{wave} by

$$E_{\mathrm{wave}} = a\, a^\star\, \omega = n\, \omega. \tag{1.119}$$

To a factor $\hbar$, the action density n can thus be interpreted as the density of wave quanta.

The wave energy density E_{wave} for each wave is derived from the general relation for the wave energy in a dispersive media:

$$E_{\mathrm{wave}} = \frac{1}{4}\left\{\epsilon_0 \vec{E}_0^\star \cdot \frac{\partial}{\partial\omega}\left[\omega\, \epsilon_H(\omega)\right] \cdot \vec{E}_0 + \frac{1}{\mu_0}\vec{H}_0^\star \cdot \frac{\partial}{\partial\omega}\left[\omega\, \mu_H(\omega)\right] \cdot \vec{H}_0\right\}, \tag{1.120}$$

where ϵ_H and μ_H are the hermitian parts of the dielectric and magnetic permeability tensors respectively, $\vec{E}_0$ and $\vec{B}_0 = \mu\vec{H}_0$ are the complex amplitudes of the electric and magnetic field components of the wave respectively, and ω is the frequency of the wave. Note, that in a plasma, the magnetic permeability tensor $\mu = \mathbf{1}$. Proof of this relation was the goal of exercise 1.2.2.2.

In the case of transverse electromagnetic waves, the dielectric tensor is given by $\epsilon = (1 - \omega_p^2/\omega^2)\mathbf{1}$, and, according to (1.84), for a given wave with wave number k and frequency ω the amplitude of the electric and magnetic fields are related to the amplitude $\mathcal{A}$ of the vector potential by

$$E_0 = i\omega\mathcal{A}, \qquad B_0 = -ik\mathcal{A},$$

so that by applying Eq. (1.120) one obtains:

$$\begin{aligned}
E_{\rm wave} &= \frac{1}{4}\left[\epsilon_0\,\omega^2|\mathcal{A}|^2\frac{\partial}{\partial\omega}\left(\omega-\frac{\omega_p^2}{\omega}\right)+\frac{1}{\mu_0}\,k^2|\mathcal{A}|^2\right]=\frac{1}{4}\epsilon_0\,\omega^2|\mathcal{A}|^2\left[1+\frac{\omega_p^2+(kc)^2}{\omega^2}\right]\\
&= \frac{1}{2}\epsilon_0\,\omega^2|\mathcal{A}|^2, \qquad (1.121)
\end{aligned}$$

having made use of the dispersion relation $\omega^2 = \omega_p^2 + (kc)^2$ for transverse waves. Comparing Eq. (1.121) with (1.119), the action amplitudes for the incident and scattered electromagnetic waves participating in the SRS mechanism are thus given respectively by:

$$a_0 = \left(\frac{\epsilon_0\,\omega_0}{2}\right)^{1/2}\mathcal{A}_0, \qquad\qquad a_s = \left(\frac{\epsilon_0\,\omega_s}{2}\right)^{1/2}\mathcal{A}_s. \qquad (1.122)$$

For EPWs, the dielectric function in the warm fluid limit considered here (see model for EPW in Sec. 1.3.2) is given by $\epsilon = 1-\omega_p^2/[\omega^2-3(kv_{\rm th})^2]$, so that for a given wave with frequency ω and amplitude $\mathcal{E}$ of the electric field, one obtains from Eq. (1.120):

$$E_{\rm wave} = \frac{1}{4}\epsilon_0\,\frac{\partial}{\partial\omega}(\omega\epsilon)\,|\mathcal{E}|^2 = \frac{1}{4}\epsilon_0\,\omega\frac{\partial\epsilon}{\partial\omega}\,|\mathcal{E}|^2 = \frac{1}{2}\epsilon_0\,\frac{\omega^2}{\omega_p^2}\,|\mathcal{E}|^2, \qquad (1.123)$$

having made use of the dispersion relation $\epsilon = 0$, i.e. $\omega^2 = \omega_p^2 + 3(kv_{\rm th})^2$, for the EPWs. Note that in this case of a longitudinal wave, there is no magnetic field contribution to the energy. Comparing Eq. (1.123) with (1.119), the action amplitude for the EPW in the SRS mechanism is thus given by:

$$a_e = \left(\frac{\epsilon_0\,\omega_e}{2}\right)^{1/2}\frac{\mathcal{E}}{\omega_p}. \qquad (1.124)$$

Inserting relations (1.122) and (1.124) into Eqs. (1.107)–(1.109), one obtains the normalized system of coupled equations for the action amplitudes of the three waves participating in SRS:

$$\begin{aligned}
\partial_t a_0 + v_{\rm g,0}\,\partial_x a_0 &= -\Gamma\,a_e\,a_s\,e^{i\delta\omega t}, &(1.125)\\
\partial_t a_s + v_{\rm g,s}\,\partial_x a_s &= +\Gamma\,a_0\,a_e^\star\,e^{-i\delta\omega t}, &(1.126)\\
\partial_t a_e + v_{\rm g,e}\,\partial_x a_e &= +\Gamma\,a_0\,a_s^\star\,e^{-i\delta\omega t}, &(1.127)
\end{aligned}$$

where one has defined the normalized coupling parameter

$$\Gamma = \frac{1}{2\sqrt{2}}\,\frac{e\,\omega_p}{m\sqrt{\epsilon_0}}\,\frac{k_e}{(\omega_0\,\omega_s\,\omega_e)^{1/2}}.$$

Note the symmetry in equations (1.125)–(1.127). Symmetry which was lacking in Eqs. (1.107)–(1.109).

The form of Eqs. (1.125)–(1.127) is now convenient for deriving conservation relations, in particular the conservation of action. Indeed, by multiplying Eqs. (1.125) by $a_0^\star$, and by multiplying the complex conjugate of Eq. (1.126) by a_s, one obtains:

$$\begin{aligned} a_0^\star\,\partial_t a_0 + v_{\mathrm{g},0}\,a_0^\star\,\partial_x a_0 &= -\Gamma\,a_0^\star\,a_s\,a_e\,e^{i\delta\omega t}, \\ a_s\,\partial_t a_s^\star + v_{\mathrm{g,s}}\,a_s\,\partial_x a_s^\star &= +\Gamma\,a_0^\star\,a_s\,a_e\,e^{i\delta\omega t}. \end{aligned}$$

Then, by adding these two equations:

$$a_0^\star\,\partial_t a_0 + v_{\mathrm{g},0}\,a_0^\star\,\partial_x a_0 + a_s\,\partial_t a_s^\star + v_{\mathrm{g,s}}\,a_s\,\partial_x a_s^\star = 0. \tag{1.128}$$

and also considering the complex conjugate of this last relation:

$$a_0\,\partial_t a_0^\star + v_{\mathrm{g},0}\,a_0\,\partial_x a_0^\star + a_s^\star\,\partial_t a_s + v_{\mathrm{g,s}}\,a_s^\star\,\partial_x a_s = 0, \tag{1.129}$$

one then finally obtains by adding Eqs. (1.128) and (1.129):

$$\partial_t|a_0|^2 + v_{\mathrm{g},0}\,\partial_x|a_0|^2 + \partial_t|a_s|^2 + v_{\mathrm{g,s}}\,\partial_x|a_s|^2 = 0,$$

which can also be written in terms of the action densities as:

$$\partial_t n_0 + \partial_x(v_{\mathrm{g},0}\,n_0) = -\left[\partial_t n_s + \partial_x(v_{\mathrm{g,s}}\,n_s)\right]. \tag{1.130}$$

Noting, that $v_{\mathrm{g},0}\,n_0$ and $v_{\mathrm{g,s}}\,n_s$ are the action fluxes for the incident and scattered waves respectively, one identifies the left hand side of Eq. (1.130) as the continuity equation for the action in the incident wave, while the right hand side corresponds to the continuity equation for action in the scattered wave. Equation (1.130) clearly states that the sink of action in the incident wave is the source of action in the scattered wave. The integral form of this local conservation law is obtained by integrating Eq. (1.130) over space, which leads to

$$\int (n_0 + n_s)\,dx = \text{const.}, \tag{1.131}$$

having assumed that waves do not propagate in or out of the system (true in particular for a periodic system).

Starting from Eqs. (1.125) and (1.127), one obtains by a similar derivation the equations for action transfer between the incident wave and the EPW, both in local form:

$$\partial_t n_0 + \partial_x(v_{\mathrm{g},0}\,n_0) = -\left[\partial_t n_e + \partial_x(v_{\mathrm{g,e}}\,n_e)\right]. \tag{1.132}$$

and in global form:

$$\int (n_0 + n_e)\,dx = \text{const.} \tag{1.133}$$

Equations (1.130)-(1.133) are the so-called Manley-Rowe relations (in local and global form). Equations (1.131) and (1.133) state that for each quantum disappearing in the incident wave, a quantum appears both in the scattered as well as in the electron plasma wave.

Together with the frequency matching condition (1.106), the Manley-Rowe equations also imply energy conservation. Indeed, multiplying Eq. (1.130) by ω_s and Eq. (1.132) by ω_e and then adding these two relations, leads to

$$(\omega_s+\omega_e)\left[\partial_t n_0+\partial_x(v_{\rm g,0}\, n_0)\right]+\omega_s\left[\partial_t n_s+\partial_x(v_{\rm g,s}\, n_s)\right]+\omega_e\left[\partial_t n_e+\partial_x(v_{\rm g,e}\, n_e)\right]=0. \quad (1.134)$$

Invoking the matching condition $\omega_0=\omega_s+\omega_e$, Eq. (1.134) can finally be written

$$\partial_t(\sum_{0,s,e} E_{\rm wave})+\partial_x(\sum_{0,s,e} v_{\rm g} E_{\rm wave})=0, \quad (1.135)$$

having made use of the relation $E_{\rm wave}=n\omega$ between the action density and wave energy density. Identifying $\sum_{0,s,e} v_{\rm g} E_{\rm wave}$ as the total energy flux from the three waves, Eq. (1.135) obviously corresponds to the local energy conservation law. The corresponding global conservation law is again obtained by integrating Eq. (1.135) over space, leading to

$$\sum_{0,s,e}\int E_{\rm wave}\, dx=\text{const}. \quad (1.136)$$

Starting from Eqs.(1.79)–(1.81), relations analog to the global (i.e. space independant) conservation laws (1.131), (1.133) and (1.136) can be derived for the system of three non-linearly coupled harmonic oscillators (see following exercise).

Exercise:

1.3.4.1 For the system of three non-linearly coupled harmonic oscillators, define the appropriate action amplitude a_j for each oscillator. Starting from Eqs. (1.79)–(1.81) for the oscillator amplitudes A_j, obtain the more symmetric set of equations for the action amplitudes a_j. Finally, derive the conservation laws for action and energy.

1.3.5 Non-Linear Analytic Solution to the Space Independent Coupling Equations

By carrying out a linear stability analysis of the three wave system (1.107)–(1.109) at the end of Sec. 1.3.2 [which is naturally equivalent to the stability analysis of the system (1.125)–(1.127)], one identified under which conditions a parametric instability may develop. One shall now consider the non-linear evolution of the three wave interaction. To facilitate the analytic derivation, one will assume that the envelopes of the waves are space independant (valid in an infinitely long or periodic system), and furthermore assume that there is no frequency mismatch. In this case, Eqs. (1.125)–(1.127) become

$$\begin{aligned}\dot{a}_1 &= -\Gamma\, a_2\, a_3, && (1.137)\\ \dot{a}_2 &= +\Gamma\, a_1\, a_3^\star, && (1.138)\\ \dot{a}_3 &= +\Gamma\, a_1\, a_2^\star, && (1.139)\end{aligned}$$

having replaced the subscripts 0, s, and e used for labeling the waves involved in the SRS mechanism by the subscripts 1, 2, and 3, so as to emphasize the generality of the following results to any set of three non-linearly interacting waves. Note that one again uses here the doted notation for time differentiation. Recall as well that Eqs. (1.137)–(1.139) have been derived under the assumption of the wave frequencies $\omega_{1,2,3}$ being all positive, which, together with the frequency matching condition $\omega_1 = \omega_2 + \omega_3$, ensures $|\omega_1| > |\omega_2|, |\omega_3|$. This is the necessary condition for possible decay of quanta from wave #1 into quanta of wave #2 and #3.

In order to derive the non-linear time evolution of the three wave amplitudes governed by Eqs. (1.137)–(1.139), one starts by expliciting the modulus α_j and phase ϕ_j for each action amplitude a_j:

$$a_j(t) = \alpha_j(t)\, e^{i\phi_j(t)}, \qquad j = 1, 2, 3. \tag{1.140}$$

Inserting (1.140) into (1.137)–(1.139), and defining the phase difference $\theta = \phi_1 - \phi_2 - \phi_3$, one obtains:

$$\begin{aligned}
\dot{\alpha_1} + i\,\alpha_1\,\dot{\phi}_1 &= -\Gamma\,\alpha_2\,\alpha_3\,e^{-i\theta},\\
\dot{\alpha_2} + i\,\alpha_2\,\dot{\phi}_2 &= +\Gamma\,\alpha_1\,\alpha_3\,e^{+i\theta},\\
\dot{\alpha_3} + i\,\alpha_3\,\dot{\phi}_3 &= +\Gamma\,\alpha_1\,\alpha_2\,e^{+i\theta}.
\end{aligned}$$

Taking the real parts of these relations provides:

$$\dot{\alpha_1} = -\Gamma\,\alpha_2\,\alpha_3\,\cos\theta, \tag{1.141}$$
$$\dot{\alpha_2} = +\Gamma\,\alpha_1\,\alpha_3\,\cos\theta, \tag{1.142}$$
$$\dot{\alpha_3} = +\Gamma\,\alpha_1\,\alpha_2\,\cos\theta, \tag{1.143}$$

and the imaginary parts:

$$\alpha_1\,\dot{\phi}_1 = \Gamma\,\alpha_2\,\alpha_3\,\sin\theta, \tag{1.144}$$
$$\alpha_2\,\dot{\phi}_2 = \Gamma\,\alpha_1\,\alpha_3\,\sin\theta, \tag{1.145}$$
$$\alpha_3\,\dot{\phi}_3 = \Gamma\,\alpha_1\,\alpha_2\,\sin\theta. \tag{1.146}$$

From Eqs. (1.141)–(1.143) one can naturally recover the Manley-Rowe relations:

$$\begin{aligned}
\frac{d}{dt}(n_1 + n_2) &= 2\,\alpha_1\,\dot{\alpha_1} + 2\,\alpha_2\,\dot{\alpha_2} = 0,\\
\frac{d}{dt}(n_1 + n_3) &= 2\,\alpha_1\,\dot{\alpha_1} + 2\,\alpha_3\,\dot{\alpha_3} = 0,
\end{aligned}$$

having used the relation $n = |a|^2 = \alpha^2$ between the action density n and the modulus α of the action amplitude a. From Eqs. (1.144)–(1.146), one can obtain an equation for the time variation of the phase difference θ:

$$\dot{\theta} = \dot{\phi}_1 - \dot{\phi}_2 - \dot{\phi}_3 = \Gamma\left(\frac{\alpha_2\alpha_3}{\alpha_1} - \frac{\alpha_1\alpha_3}{\alpha_2} - \frac{\alpha_1\alpha_2}{\alpha_3}\right)\sin\theta,$$

and making again use of Eqs. (1.141)–(1.143) one can further write:

$$\dot{\theta} = -\left(\frac{\dot{\alpha}_1}{\alpha_1} + \frac{\dot{\alpha}_2}{\alpha_2} + \frac{\dot{\alpha}_3}{\alpha_3}\right) \tan\theta = -\tan\theta \,\frac{d}{dt} \ln(\alpha_1\, \alpha_2\, \alpha_3),$$

which leads to another invariant quantity:

$$\frac{\dot{\theta}}{\tan\theta} = -\frac{d}{dt} \ln(\alpha_1\, \alpha_2\, \alpha_3) \qquad \Longrightarrow \qquad \frac{d}{dt} \ln(\alpha_1\, \alpha_2\, \alpha_3\, \sin\theta) = 0.$$

The invariants for the system (1.137)–(1.139) can thus be summarized as follows:

$$\begin{aligned} n_1 + n_2 &= \text{const.} \doteq m_2, & (1.147)\\ n_1 + n_3 &= \text{const.} \doteq m_3, & (1.148)\\ \alpha_1\, \alpha_2\, \alpha_3\, \sin\theta &= \text{const.} \doteq C. & (1.149) \end{aligned}$$

These constants are now used in deriving the non-linear time evolution of the spatially uniform action densities n_j. Starting from Eq. (1.141), one computes the time variation of n_1:

$$\dot{n}_1 = 2\,\alpha_1\,\dot{\alpha}_1 = -2\,\Gamma\,\alpha_1\,\alpha_2\,\alpha_3\,\cos\theta.$$

Writing $\cos\theta = \pm(1 - \sin^2\theta)^{1/2}$ and making use of Eq. (1.149) then leads to:

$$\dot{n}_1 = \pm\, 2\,\Gamma\,\alpha_1\,\alpha_2\,\alpha_3 \left(1 - \frac{C^2}{\alpha_1^2\,\alpha_2^2\,\alpha_3^2}\right)^{1/2} = \pm\, 2\,\Gamma\,(n_1\, n_2\, n_3 - C^2)^{1/2}.$$

Finally, one invokes the invariants given by Eqs. (1.147) and (1.148) to obtain:

$$\dot{n}_1 = \pm\, 2\,\Gamma\, \left[n_1\,(m_2 - n_1)\,(m_3 - n_1) - C^2\right]^{1/2}.$$

This last equation depends only on n_1 and can thus be solved by quadrature:

$$\underbrace{\frac{1}{2}\int_{n_1(t_0)}^{n_1(t)} \frac{dn_1}{\left[n_1\,(m_2 - n_1)\,(m_3 - n_1) - C^2\right]^{1/2}}}_{I} = \pm\,\Gamma\,(t - t_0), \tag{1.150}$$

where for now, t_0 represents an arbitrary reference time. The integral I on the left hand side of Eq. (1.150) is an elliptic integral [5], and can in fact be expressed in terms of the elliptic integral of the first kind, as is now shown. For this one notes n_a, n_b and n_c the roots of the cubic equation

$$n_1\,(m_2 - n_1)\,(m_3 - n_1) - C^2 = 0. \tag{1.151}$$

These roots can be ordered such that

$$0 \le n_a \le n_b \le n_c. \tag{1.152}$$

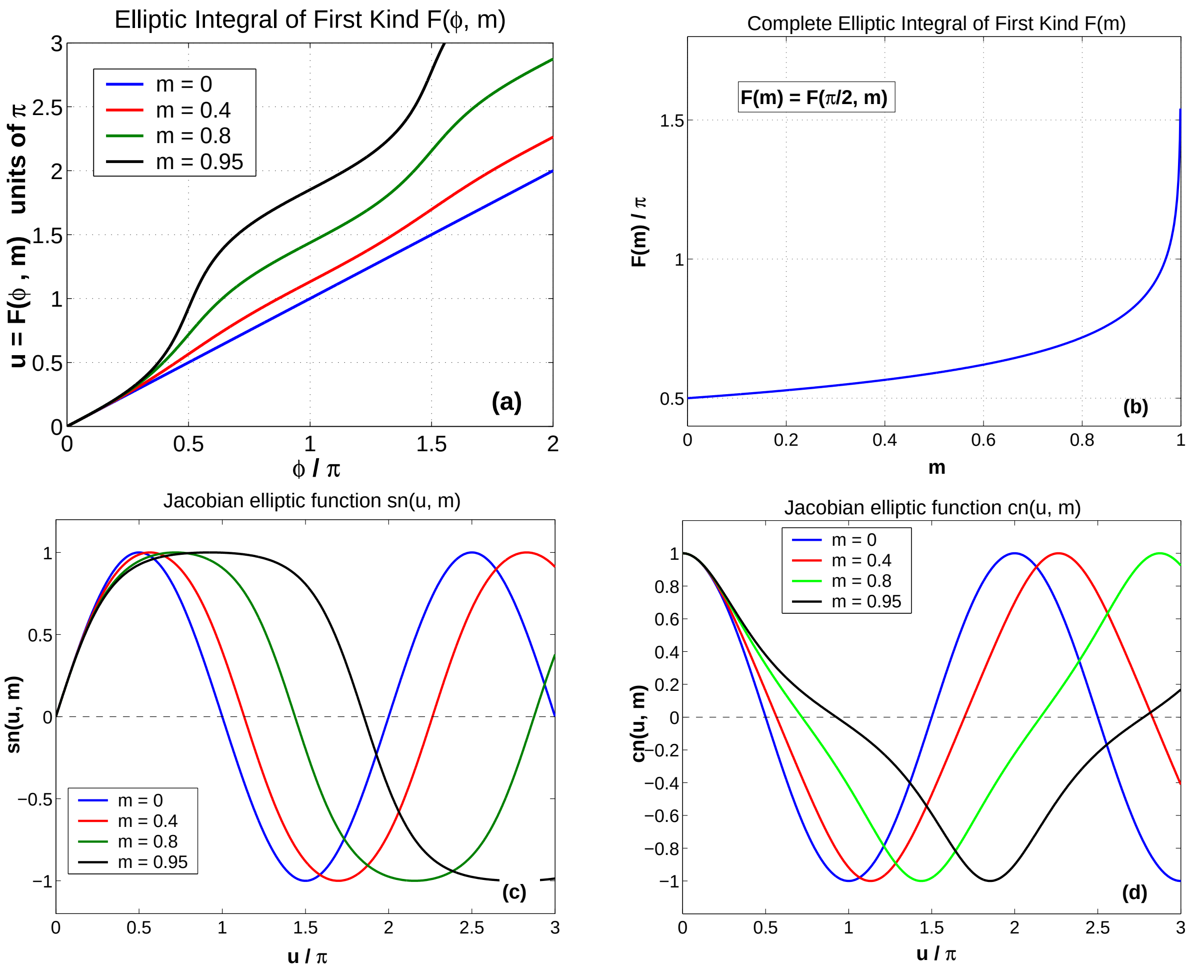

Figure 1.13: (a) Elliptic integral of the first kind $F(\varphi, m)$. (b) Complete elliptic integral of the first kind $F(m) = F(\pi/2, m)$. (c) Jacobian elliptic function $\mathrm{sn}(u, m)$. (d) Jacobian elliptic function $\mathrm{cn}(u, m)$.

The integral I can thus be written:

$$I = \frac{1}{2}\int_{n_1(t_0)}^{n_1(t)} \frac{dn_1}{\left[(n_1 - n_a)(n_1 - n_b)(n_1 - n_c)\right]^{1/2}}.$$

By further making the change of variables

$$y = \left(\frac{n_1 - n_a}{n_b - n_a}\right)^{1/2}, \tag{1.153}$$

one obtains (check it):

$$I = \frac{1}{(n_c - n_a)^{1/2}}\int_0^{y(t)} \frac{dy}{\left[(1-y^2)(1-\mu^2 y^2)\right]^{1/2}} = \frac{1}{(n_c - n_a)^{1/2}}\, F[\arcsin y(t), \mu^2], \tag{1.154}$$

having defined the parameter

$$\mu^2 = \frac{n_b - n_a}{n_c - n_a}, \tag{1.155}$$

which, as a result from the ordering (1.152), is such that $0 \le \mu^2 \le 1$. To obtain the first equality in (1.154), one has now defined the time t_0 such that

$$n_1(t_0) = n_a,$$

which led to the lower boundary of the integral in y being equal to zero. The second equality in (1.154) was obtained using the definition of the elliptic integral of the first kind [5]:

$$F(\varphi, m) = \int_0^{\varphi} \frac{d\theta}{(1 - m\sin^2\theta)^{1/2}} = \int_0^{\sin\varphi} \frac{dx}{\left[(1-x^2)(1-mx^2)\right]^{1/2}},$$

with $x = \sin\theta$, and $0 \le m \le 1$.

Inserting (1.154) into (1.150) gives then:

$$F[\arcsin y(t), \mu^2] = \pm\,(n_c - n_a)^{1/2}\,\Gamma\,(t - t_0).$$

This last relation can be inverted for $y(t)$:

$$y(t) = \pm\,\mathrm{sn}\left[(n_c - n_a)^{1/2}\,\Gamma\,(t - t_0), \mu^2\right]. \tag{1.156}$$

Here $\mathrm{sn}(u, m)$, $0 \le m \le 1$, is one of the Jacobian elliptic functions defined by

$$u = F(\varphi, m) \quad \Longleftrightarrow \quad \mathrm{sn}(u, m) = \sin\varphi. \tag{1.157}$$

Note that one has $\mathrm{sn}(u, m = 0) = \sin u$, and for $0 < m < 1$ the elliptic function $\mathrm{sn}(u, m)$ appears as a "flattened" sin function (see Fig. 1.13). Let us immediately introduce here $\mathrm{cn}(u, m)$, which is another Jacobian elliptic function, defined by

$$u = F(\varphi, m) \quad \Longleftrightarrow \quad \mathrm{cn}(u, m) = \cos\varphi. \tag{1.158}$$

Comparing definitions (1.157) and (1.158) for $\mathrm{sn}(u,m)$ and $\mathrm{cn}(u,m)$ respectively, one obviously has the relation $\mathrm{sn}^2(u,m)+\mathrm{cn}^2(u,m) = 1$ for any argument u and parameter $0 \leq m \leq 1$.

Now, inserting (1.156) into (1.153) finally provides the solution for the action density of wave #1:

$$n_1(t) = n_a + (n_b - n_a)\,\mathrm{sn}^2\left[(n_c-n_a)^{1/2}\,\Gamma\,(t-t_0),\mu^2\right]. \tag{1.159}$$

Note that $n_1(t)$ oscillates between the values n_a and n_b with period $T = 2F(\mu^2)/[\Gamma(n_c - n_a)^{1/2}]$, where $F(m) = F(\pi/2, m)$ is the complete elliptic integral of the first kind, and that one indeed has $n_1(t_0) = n_a$.

The time evolution of the action densities for wave #2 and #3 are then simply obtained from (1.147) and (1.148):

$$n_2(t) = m_2 - n_1(t) = (m_2 - n_b) + (n_b-n_a)\,\mathrm{cn}^2\left[(n_c-n_a)^{1/2}\,\Gamma\,(t-t_0),\mu^2\right], \tag{1.160}$$

$$n_3(t) = m_3 - n_1(t) = (m_3 - n_b) + (n_b-n_a)\,\mathrm{cn}^2\left[(n_c-n_a)^{1/2}\,\Gamma\,(t-t_0),\mu^2\right]. \tag{1.161}$$

Equations (1.159)–(1.161) clearly provide solutions for the action densities of the three waves in terms of the initial conditions. Note in particular, that the values n_a, n_b and n_c, being solution of Eq. (1.151), are function of the invariants of motion m_2, m_3 and C, and thus function of the initial conditions of the system.

One now considers the solutions (1.159)–(1.161) for the action densities of the three nonlinearly coupled waves in two particular cases of initial conditions.

Case 1. $n_3(0) \gg n_2(0) > n_1(0) = 0$.

For these initial conditions, the invariants (1.147)–(1.149) become

$$\begin{aligned} m_2 &= n_1(0)+n_2(0) = n_2(0),\\ m_3 &= n_1(0)+n_3(0) = n_3(0),\\ C &= [n_1(0)\,n_2(0)\,n_3(0)]^{1/2}\sin[\theta(0)] = 0. \end{aligned}$$

The properly ordered roots $n_{a,b,c}$ to the cubic equation (1.151) thus are given by

$$[n_a = 0] \;<\; [n_b = m_2 = n_2(0)] \;<\; [n_c = m_3 = n_3(0)],$$

and the parameter $\mu^2 = n_2(0)/n_3(0) \ll 1$, so that $\mathrm{sn}(u,\mu^2) \simeq \sin(u)$.

In this case, the solutions (1.159)-(1.161) can be written

$$n_1(t) \simeq n_2(0)\,\sin^2[\sqrt{n_3(0)}\,\Gamma\,t], \tag{1.162}$$

$$n_2(t) \simeq n_2(0)\,\cos^2[\sqrt{n_3(0)}\,\Gamma\,t], \tag{1.163}$$

$$n_3(t) \simeq n_3(0) - n_2(0)\,\sin^2[\sqrt{n_3(0)}\,\Gamma\,t]. \tag{1.164}$$

This scenario is plotted in figure 1.14.a. It clearly illustrates stability in the case for which the frequency of the large amplitude wave (here wave # 3) is lower than at least one of the frequencies of the two other waves.

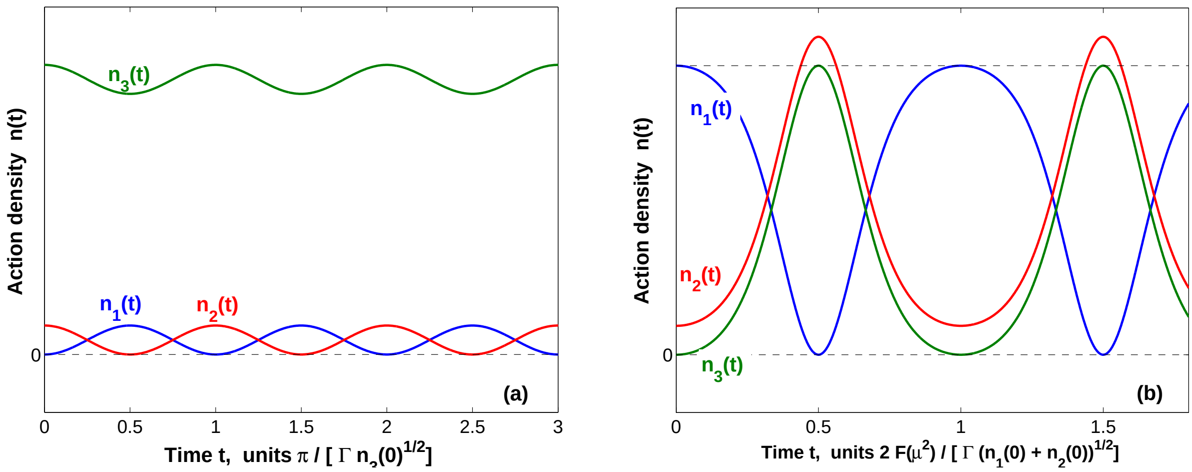

Figure 1.14: Time evolution of the action densities for the three non-linearly coupled waves in the case where the initially finite amplitude wave has a frequency (a) smaller than at least one of the frequencies of the two other waves, (b) larger than the two other frequencies.

Case 2. $n_1(0) \gg n_2(0) > n_3(0) = 0$**.**

For these initial conditions, the invariants (1.147)–(1.149) are given by

$$\begin{aligned} m_2 &= n_1(0) + n_2(0), \\ m_3 &= n_1(0), \\ C &= 0, \end{aligned}$$

and the properly ordered roots $n_{a,b,c}$ to Eq. (1.151) by

$$[n_a = 0] \; < \; [n_b = m_3 = n_1(0)] \; < \; [n_c = m_2 = n_1(0) + n_2(0)],$$

so that the parameter $\mu^2 = n_1(0)/[n_1(0) + n_2(0)] \simeq 1$.

In this case, the solutions (1.159)–(1.161) can thus be written

$$n_1(t) = n_1(0)\,\mathrm{sn}^2\left[\sqrt{n_1(0) + n_2(0)}\,\Gamma\,(t - t_0), \mu^2\right], \tag{1.165}$$

$$n_2(t) = n_2(0) + n_1(0)\,\mathrm{cn}^2\left[\sqrt{n_1(0) + n_2(0)}\,\Gamma\,(t - t_0), \mu^2\right], \tag{1.166}$$

$$n_3(t) = n_1(0)\,\mathrm{cn}^2\left[\sqrt{n_1(0) + n_2(0)}\,\Gamma\,(t - t_0), \mu^2\right], \tag{1.167}$$

where $t_0 = F(\mu^2)/\Gamma\,[n_1(0) + n_2(0)]^{1/2}$, so that one indeed has $n_1(t = 0) = n_1(0)$.

This scenario is plotted in figure 1.14.b. It corresponds to the unstable case where the frequency of the large amplitude wave (here wave # 1) is larger than the frequencies of the two other waves. This result illustrates the most obvious saturation mechanism for the parametric instability: Depletion of the pump. Indeed, once there is no more energy in the pump wave, the instability clearly stops to grow. The saturation time is given by $t_0 \sim 1/\gamma = 1/[\Gamma\, n_1(0)^{1/2}]$, i.e. scales as the inverse of the growth rate γ obtained from the linear stability analysis of system (1.137)–(1.139) in the case $|a_1| \gg |a_2|, |a_3|$.

The oscillatory nature of solution (1.165)–(1.167) furthermore points out that the decay of quanta from wave #1 into quanta of wave #2 and #3 is in fact reversible.

1.3.6 Saturation Mechanisms

Pump depletion turns out to be the only saturation mechanism included in the simple fluid model for the three wave interaction considered in the previous sections. In reality many other saturation mechanisms, involving additional waves and/or kinetic effects, may potentially play a role. In the case of SRS for example, let us point out the following saturation processes:

- As the SRS instability develops and the amplitude of the EPW increases, a non-linear frequency shift of this wave may be induced (see Sec. 1.2.6). This frequency shift thus leads to a frequency mismatch of the three wave interaction, and, according to Eq. (1.114), to a less efficient growth of the parametric instability.
- SRS may saturate as a result of the EPW, generated by parametric instability, undergoing a secondary instability once it reached a certain amplitude threshold: The so-called Langmuir Decay Instability (LDI, see exercise 1.3.3.2), in which the primary EPW decays into another EPW and an IAW.
- The EPW may also be subject to another type of secondary instability once its amplitude is such that the wave has trapped a significant fraction of electrons: The Trapped Particle Instability (TPI, see Sec. 1.2.7) [17].

1.3.7 Illustrations from Simulations

Bursting behavior of SRS

Raman Amplifier

1.3.8 Further Reading

- **Parametric instabilities in laser plasma interaction (LPI)**: See the excellent introductory book by Kruer [13].
- **Parametric instability in magnetized plasma**: See illustration in Sec. 2 of Chap. I of Ref. [1] treating the case of coupling between Alvén and sound waves.
- **Parametric instabilities in inhomogeneous plasmas**: Article by Rosenbluth [14].
- **Systematic study of parametric instabilities affecting EM waves in plasmas**: See the much referenced article by Drake *et. al* [15].

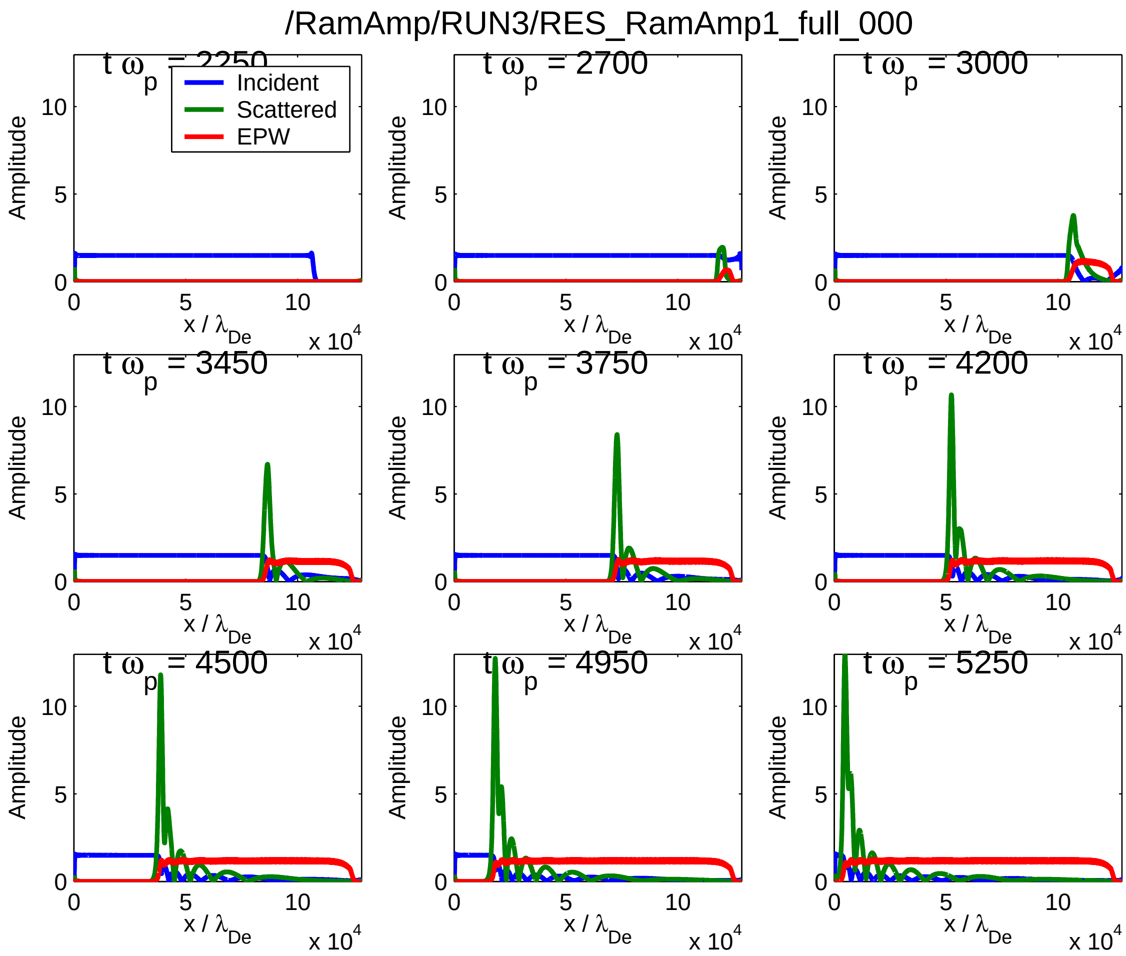
/RamAmp/RUN3/RES_RamAmp1_full_000
t ω_p = 2250
t ω_p = 2700
t ω_p = 3000
t ω_p = 3450
t ω_p = 3750
t ω_p = 4200
t ω_p = 4500
t ω_p = 4950
t ω_p = 5250
Incident
Scattered
EPW
Amplitude
x / λ_De
x 10^4

- **Simulations**: See for example Vu *et. al* [16] as an example for PIC-type simulations, and Johnston *et. al* and Brunner & Valeo [17] as examples of Eulerian-type calculations.

- **Raman amplifiers**: For theory see work by Shvets, Fish, Malkin *et. al* [18, 19], for simulation results the thesis by Clark [20], and for experimental results see the work by Ping [21].

Appendix A

Particles in a Sinusoidal Potential

A.1 Trapped and Untrapped Particles

One considers here the trajectories of electrons in a sinusoidal wave $E(x,t) = E_0 \sin(k_0 x - \omega_0 t)$. One notes that the electrons moving in the field E are separated into two groups: Passing and trapped. This is clearly seen by working in the frame of reference moving with the wave, i.e. at velocity $v_\phi = \omega_0/k_0$ with respect to the lab frame. In this wave frame, the electrostatic field becomes $E = E_0 \sin(k_0 x) = -\partial\phi/\partial x$, with the potential $\phi = (E_0/k_0)\cos(k_0 x)$, so that the total energy of an electron is given by

$$W = \frac{1}{2} m\, v^2 - \frac{eE_0}{k_0} \cos(k_0 x). \tag{A.1}$$

If one assumes the amplitude E_0 to be time independent, the energy W is conserved for each particle. As illustrated in Fig. A.1, electrons with energy levels $-eE_0/k_0 < W < eE_0/k_0$ are trapped, while particles with energy levels $W > eE_0/k_0$ are untrapped. The terms "untrapped" and "passing" are used interchangeably.

A.2 Deeply Trapped Particles

To start, one considers the case of electrons with energies near $W_{\min} = -eE_0/k_0$, which remain at the bottom of the potential wells, i.e. around the positions $x_{\min} = n\lambda_0 = n\, 2\pi/k_0$, n integer. These are the so-called deeply trapped particles. By expanding the potential to second order at the bottom of the well, the total energy (A.1) can be written

$$W = \frac{1}{2} m\, v^2 + \frac{1}{2} e k_0 E_0 (x - x_{\min})^2 + \text{const},$$

which is simply the energy of a harmonic oscillator with frequency $\omega_b = (e k_0 E_0/m)^{1/2}$, the so-called deeply trapped bounce frequency.

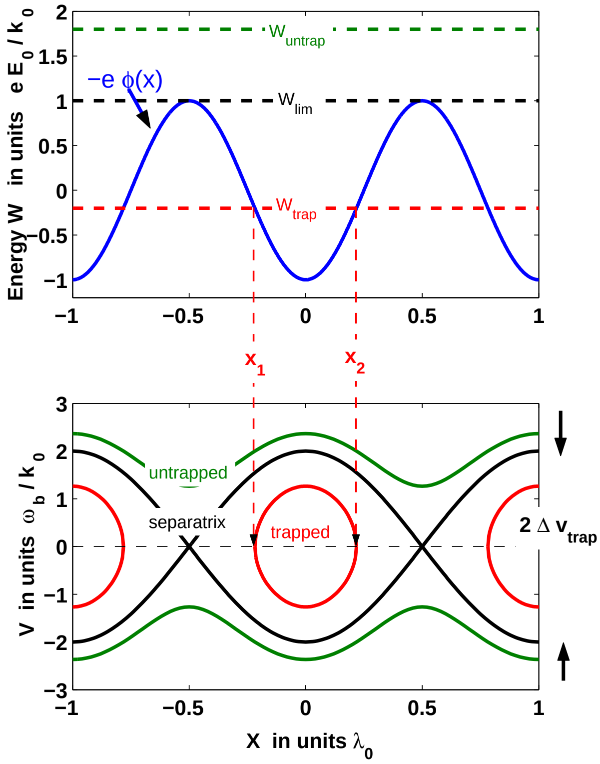

Figure A.1: a) Sinusoidal potential $-e\phi(x)$ in wave frame. b) Untrapped and trapped orbits of particles.

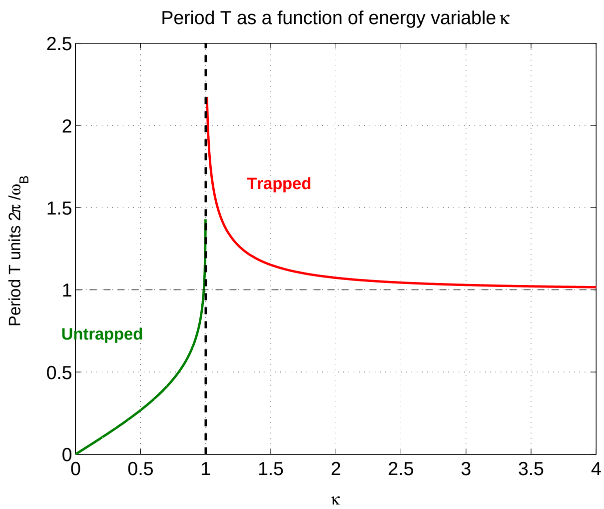

Figure A.2: Transit time and bounce period of particles in a sinusoidal potential as a function of the energy variable κ.

A.3 General Case of Untrapped Particles

One now considers the case of untrapped electrons in a sinusoidal wave with no further assumption. From Eq. (A.1), one obtains

$$v(x, W) = \left[\frac{2}{m}\left(W + \frac{eE_0}{k_0}\cos(k_0 x)\right)\right]^{1/2} = \frac{\Delta v_{\text{trap}}}{\kappa}(1 - \kappa^2 \sin^2\xi)^{1/2}, \tag{A.2}$$

having defined $\xi = k_0 x/2$, as well as the transformed energy variable

$$\kappa^2 = \frac{2eE_0}{k_0 W + eE_0}. \tag{A.3}$$

Here one has also made use of the notation $\Delta v_{\text{trap}} = 2\omega_b/k_0$ for the trapping width in velocity (see Fig. A.1). In terms of κ, the passing condition becomes $0 < \kappa < 1$.

The transit time τ_t, i.e. the time required for an untrapped particle to cover one period $\lambda_0 = 2\pi/k_0$, is derived as follows

$$\tau_t(\kappa) = \int_{-\lambda_0/2}^{\lambda_0/2} \frac{dx}{v(x,\kappa)} = \frac{\kappa}{\Delta v_{\text{trap}}}\frac{2}{k_0}\int_{-\pi/2}^{\pi/2}\frac{d\xi}{(1-\kappa^2\sin^2\xi)^{1/2}} = \frac{2\kappa}{\omega_b}F(\kappa^2), \tag{A.4}$$

where $F(m) = \int_0^{\pi/2} d\theta/(1 - m\sin^2\theta)^{1/2}$, $0 < m < 1$, is the complete elliptic integral of the first kind [5]. The transit time τ_t is plotted as a function of κ in Fig. A.2. Note how τ_t becomes infinite in the limit $\kappa \to 1-$, i.e. for marginally passing particles.

The space averaged velocity is another useful quantity:

$$\begin{aligned}
\bar{v}(\kappa) = < v >_x &= \frac{1}{\lambda_0}\int_{-\lambda_0/2}^{\lambda_0/2} dx\, v(x,\kappa) = \frac{\Delta v_{\text{trap}}}{\kappa}\frac{2}{\lambda_0 k_0}\int_{-\pi/2}^{\pi/2} d\xi\,(1-\kappa^2\sin^2\xi)^{1/2} \\
&= \frac{2}{\pi}\frac{\Delta v_{\text{trap}}}{\kappa}E(\kappa^2),
\end{aligned} \tag{A.5}$$

where $E(m) = \int_0^{\pi/2} d\theta(1 - m\sin^2\theta)^{1/2}$, $0 < m < 1$, is the complete elliptic integral of the second kind [5].

A.4 General Case of Trapped Particles

Here one treats the case of trapped electrons which are not necessarily deeply trapped. Noting that equation (A.2) is still valid here, and that in terms of κ the trapping condition becomes $\kappa > 1$, the bounce period τ_b is derived as follows:

$$\begin{aligned}
\tau_b(\kappa) &= 2\int_{x_1}^{x_2}\frac{dx}{v(x,\kappa)} = 2\frac{\kappa}{\Delta v_{\text{trap}}}\frac{2}{k_0}\int_{\xi_1}^{\xi_2}\frac{d\xi}{(1-\kappa^2\sin^2\xi)^{1/2}} \\
&= \frac{2}{\omega_b}\int_{-\pi/2}^{\pi/2}\frac{d\eta}{(1-\frac{1}{\kappa^2}\sin^2\eta)^{1/2}} = \frac{4}{\omega_b}F(\frac{1}{\kappa^2}),
\end{aligned} \tag{A.6}$$

where the turning points $x_{1,2} = 2\xi_{1,2}/k_0$ verify $\cos(k_0 x_{1,2}) = -k_0 W/eE_0 \Longleftrightarrow \kappa \sin\xi_{1,2} = \pm 1$. One has also made use here of the change of variables $\xi \leftrightarrow \eta$ defined by $\kappa \sin\xi = \sin\eta$, so that $\kappa d\xi/(1-\kappa^2\sin^2\xi)^{1/2} = d\eta/(1-\sin^2\eta/\kappa^2)^{1/2}$. Note that in deriving (A.6) one took account of both the time for the forward and backward segment of the trapped particle orbit [factor 2 in first equality of relation(A.6)]. The bounce period τ_b is also plotted as a function of κ in Fig. A.2. In the limit $\kappa \to 1+$, i.e. for marginally trapped particles, τ_b becomes infinite.

Deeply trapped particles correspond to $\kappa \to \infty$, so that, as expected, one recovers from Eq.(A.6) the bounce period for deeply trapped particles derived previously: $\tau_b^{\text{deep}} = \lim_{\kappa\to\infty} \tau_b = 2\pi/\omega_b$, having used $F(0) = \pi/2$.

The space averaged velocity is again obtained in a similar way:

$$\begin{aligned}
\bar{v}(\kappa) = < v >_x &= \frac{1}{\lambda_0}\int_{x_1}^{x_2} dx\, v(x,\kappa) = \frac{\Delta v_{\text{trap}}}{\kappa}\frac{2}{\lambda_0 k_0}\int_{\xi_1}^{\xi_2} d\xi\,(1-\kappa^2\sin^2\xi)^{1/2} \\
&= \frac{\Delta v_{\text{trap}}}{\pi\kappa^2}\int_{-\pi/2}^{\pi/2} d\eta \frac{\cos^2\eta}{(1-\frac{1}{\kappa^2}\sin^2\eta)^{1/2}} \\
&= \frac{2\Delta v_{\text{trap}}}{\pi}\left[E(\frac{1}{\kappa^2}) + (\frac{1}{\kappa^2}-1)F(\frac{1}{\kappa^2})\right],
\end{aligned} \tag{A.7}$$

having used $\cos^2\eta = (1-\kappa^2) + \kappa^2(1-\sin^2\eta/\kappa^2)$ for obtaining the final relation.

Appendix B

Solving the (Linearized) Vlasov Equation by Integrating Along Trajectories

One discusses here the general approach to solving the non-linear Vlasov equation or its linearized form. One thus considers the Vlasov equation for the distribution $f(\vec{x}, \vec{v}, t)$ in phase space $(\vec{x}, \vec{v})$ of a given species with charge q and mass m evolving in the electromagnetic fields $[\vec{E}(\vec{x}, t), \vec{B}(\vec{x}, t)]$:

$$\frac{\partial f}{\partial t} + \vec{v} \cdot \frac{\partial f}{\partial \vec{x}} + \frac{q}{m} \left(\vec{E} + \vec{v} \times \vec{B} \right) \cdot \frac{\partial f}{\partial \vec{v}} = 0. \tag{B.1}$$

To lighten notations in the following, one writes $\vec{F} = q(\vec{E} + \vec{v} \times \vec{B})$ the total force on the particles.

B.1 Brief Review of the Vlasov Equation

Let us recall, that the Vlasov equation results from the incompressibility of phase space flux $\vec{V}(\vec{z}, t) = [\vec{v}, \vec{F}(\vec{x}, \vec{v}, t)/m]$, which in general is a 6-dimensional vector in phase space $\vec{z} = (\vec{x}, \vec{v})$. This is briefly reviewed here.

Indeed, if the total number of particles remains constant (no sources or sinks for the considered species, such as ionization or recombination processes), one can write a continuity equation for the phase space density $f(\vec{x}, \vec{v}, t)$ of particles:

$$\frac{\partial f}{\partial t} + \frac{\partial}{\partial \vec{z}} \cdot (\vec{V} f) = \frac{\partial f}{\partial t} + \frac{\partial}{\partial \vec{x}} \cdot (\vec{v} f) + \frac{\partial}{\partial \vec{v}} \cdot (\frac{\vec{F}}{m} f) = 0. \tag{B.2}$$

One notes that for the considered electromagnetic forces $\vec{F}$, related to the macroscopic fields $(\vec{E}, \vec{B})$, the phase space flux $\vec{V}$ is such that:

$$\frac{\partial}{\partial \vec{z}} \cdot \vec{V} = \underbrace{\frac{\partial}{\partial \vec{x}} \cdot \vec{v}}_{=0} + \underbrace{\frac{\partial}{\partial \vec{v}} \cdot \frac{q}{m}(\vec{E} + \vec{v} \times \vec{B})}_{=0} = 0, \tag{B.3}$$

having in particular used the fact that $\vec{E}(\vec{x}, t)$ is velocity independent, and

$$\frac{\partial}{\partial \vec{v}} \cdot (\vec{v} \times \vec{B}) = \vec{B} \cdot \underbrace{(\frac{\partial}{\partial \vec{v}} \times \vec{v})}_{=0} - \vec{v} \cdot \underbrace{(\frac{\partial}{\partial \vec{v}} \times \vec{B})}_{=0} = 0.$$

Equation (B.3) describes the incompressibility of phase space flux $\vec{V}$.

As a result of relation (B.3), the continuity equation (B.2) becomes:

$$\frac{\partial f}{\partial t} + \frac{\partial}{\partial \vec{z}} \cdot (\vec{V} f) = \frac{\partial f}{\partial t} + \underbrace{(\frac{\partial}{\partial \vec{z}} \cdot \vec{V})}_{=0} f + \vec{V} \cdot \frac{\partial f}{\partial \vec{z}} = 0.$$

This last relation clearly provides Vlasov's equation (B.1).

Vlasov's equation in fact states that the distribution f remains invariant along the particle trajectories in phase space, which naturally again reflects phase space incompressibility. One can indeed write Eq. (B.1) as

$$\left.\frac{df}{dt}\right|_{\text{traj.}} = 0, \tag{B.4}$$

where $d/dt|_{\text{traj}}$ is the total time derivative along the trajectories. To convince oneself that Eq. (B.4) is equivalent to the Vlasov equation, one considers the trajectory $[\vec{x}\,'(t'), \vec{v}\,'(t')]$ in phase space of any given particle. This trajectory must verify the equations of motion:

$$\frac{d\vec{x}\,'(t')}{dt'} = \vec{v}\,'(t'), \tag{B.5}$$

$$\frac{d\vec{v}\,'(t')}{dt'} = \frac{q}{m} \vec{F}[\vec{x}\,'(t'), \vec{v}\,'(t'), t']. \tag{B.6}$$

The value of the distribution along the particle trajectory, i.e. $f[\vec{x}\,'(t'), \vec{v}\,'(t'), t']$, is function of the single variable t'. The variation in time of this function is thus:

$$\begin{aligned} \frac{d}{dt'} f[\vec{x}\,'(t'), \vec{v}\,'(t'), t'] &= \frac{\partial f(\vec{x}\,', \vec{v}\,', t')}{\partial t'} + \frac{d\vec{x}\,'}{dt'} \cdot \frac{\partial f(\vec{x}\,', \vec{v}\,', t')}{\partial \vec{x}\,'} + \frac{d\vec{v}\,'}{dt'} \cdot \frac{\partial f(\vec{x}\,', \vec{v}\,', t')}{\partial \vec{v}\,'} \\ &= \left.\left[\frac{\partial f}{\partial t} + \vec{v} \cdot \frac{\partial f}{\partial \vec{x}} + \frac{\vec{F}(\vec{x}, \vec{v}, t)}{m} \cdot \frac{\partial f}{\partial \vec{v}} \right]\right|_{(\vec{x}\,', \vec{v}\,', t')} = 0, \end{aligned} \tag{B.7}$$

having used Eqs.(B.5)-(B.6) and the Vlasov equation (B.1). This last result clearly proves Eq. (B.4), and validates the notation for the Vlasov operator:

$$\left.\frac{d}{dt}\right|_{\text{traj.}} = \frac{\partial}{\partial t} + \vec{v} \cdot \frac{\partial}{\partial \vec{x}} + \frac{\vec{F}}{m} \cdot \frac{\partial}{\partial \vec{v}}.$$

B.2 Solving the Vlasov Equation

One considers solving the full Vlasov equation

$$\left.\frac{df}{dt}\right|_{\text{traj.}} = \frac{\partial f}{\partial t} + \vec{v} \cdot \frac{\partial f}{\partial \vec{x}} + \frac{\vec{F}}{m} \cdot \frac{\partial f}{\partial \vec{v}} = 0,$$

for the initial condition

$$f(\vec{x}, \vec{v}, 0) = f_0(\vec{x}, \vec{v}).$$

Formally at least, the solution $f(\vec{x}, \vec{v}, t)$ can be written in terms of the particle trajectories, by invoking the invariance of f along these characteristics. Indeed, by integrating (B.7) between time $t' = 0$ and $t' = t$ for the trajectory $[\vec{x}\,'(t'; \vec{x}, \vec{v}, t), \vec{v}\,'(t'; \vec{x}, \vec{v}, t)]$ verifying the particular initial conditions:

$$\vec{x}\,'(t' = t) = \vec{x}, \qquad \text{and} \qquad \vec{v}\,'(t' = t) = \vec{v},$$

one simply obtains:

$$f(\vec{x}, \vec{v}, t) - f_0[\vec{x}\,'(0; \vec{x}, \vec{v}, t), \vec{v}\,'(0; \vec{x}, \vec{v}, t)] = \int_0^t dt' \frac{d}{dt'} f[\vec{x}\,'(t'), \vec{v}\,'(t'), t'] = 0,$$

$$\Longrightarrow \quad f(\vec{x}, \vec{v}, t) = f_0[\vec{x}\,'(0; \vec{x}, \vec{v}, t), \vec{v}\,'(0; \vec{x}, \vec{v}, t)].$$

One must however point out here, that computing the trajectories $(\vec{x}\,', \vec{v}\,')$ may not be straightforward, as the electromagnetic forces $\vec{F} = q(\vec{E} + \vec{v} \times \vec{B})$ determining these trajectories are themselves function of f [the plasma itself provides sources to the electromagnetic fields $(\vec{E}, \vec{B})$]. This issue reflects the non-linear nature of the plasma.

B.3 Solving the Linearized Vlasov Equation

The method of integrating along particle trajectories can also be applied when solving the linearized Vlasov equation. Let us assume that $(f_0, \vec{E}_0, \vec{B}_0)$ is a known unperturbed state of the Vlasov-Maxwell system. Note that this state need not be necessarily time independent. In particular, Vlasov's equation reads

$$\left.\frac{df_0}{dt}\right|_{\text{u.traj.}} = \left[\frac{\partial}{\partial t} + \vec{v} \cdot \frac{\partial}{\partial \vec{x}} + \frac{\vec{F}_0}{m} \cdot \frac{\partial}{\partial \vec{v}}\right] f_0 = 0,$$

where $(d/dt)|_{\text{u.traj.}}$ stands for the total time derivative along the *unperturbed* trajectories in the force field $\vec{F}_0 = q(\vec{E}_0 + \vec{v} \times \vec{B}_0)$.

One now considers a perturbation $(\delta f, \delta\vec{E}, \delta\vec{B})$ to this state. The Vlasov equation for the full distribution $f = f_0 + \delta f$ reads

$$\left.\frac{df}{dt}\right|_{\text{traj.}} = \left[\frac{\partial}{\partial t} + \vec{v} \cdot \frac{\partial}{\partial \vec{x}} + \frac{\vec{F}_0 + \delta\vec{F}}{m} \cdot \frac{\partial}{\partial \vec{v}}\right] (f_0 + \delta f) = 0, \tag{B.8}$$

where $(d/dt)|_{\text{traj.}}$ stands for the total time derivative along the trajectories in the *full* (i.e. including perturbations) force field $\vec{F} = \vec{F} + \delta\vec{F}$, with $\delta\vec{F} = q(\delta\vec{E} + \vec{v} \times \delta\vec{B})$. Assuming small amplitude perturbation, one can justify linearizing Eq. (B.8), which leads to the linearized Vlasov equation for δf:

$$\left.\frac{d\delta f}{dt}\right|_{\text{u.traj.}} = \left[\frac{\partial}{\partial t} + \vec{v}\cdot\frac{\partial}{\partial \vec{x}} + \frac{\vec{F}_0}{m}\cdot\frac{\partial}{\partial \vec{v}}\right]\delta f = -\frac{\delta\vec{F}}{m}\cdot\frac{\partial f_0}{\partial \vec{v}}, \tag{B.9}$$

noting that on the left hand side of Eq. (B.9) one finds again the total time derivative along the unperturbed trajectories. Note, that as a result of the non-zero right hand side term in Eq. (B.9), δf is not invariant along the unperturbed trajectories. Only the full distribution $f = f_0 + \delta f$ is invariant along the full trajectories as stated by Eq. (B.8).

Equation (B.9) can nonetheless be solved for δf by integrating along trajectories. The non-zero right hand side provides however an additional contribution. Indeed, by evaluating Eq. (B.9) along an *unperturbed trajectory* $[\vec{x}\,'(t';\vec{x},\vec{v},t), \vec{v}\,'(t';\vec{x},\vec{v},t)]$, and integrating again from time $t'=0$ to $t'=t$, one obtains:

$$\begin{aligned}
\delta f(\vec{x},\vec{v},t) - \delta f_0[\vec{x}\,'(0;\vec{x},\vec{v},t),\vec{v}\,'(0;\vec{x},\vec{v},t)] &= \int_0^t dt' \frac{d}{dt'}\delta f[\vec{x}\,'(t'),\vec{v}\,'(t'),t'] \\
&= -\int_0^t dt' \left.\frac{\delta\vec{F}}{m}\cdot\frac{\partial f_0}{\partial\vec{v}}\right|_{(\vec{x}\,',\vec{v}\,',t')},
\end{aligned}$$

$$\Longrightarrow \quad \delta f(\vec{x},\vec{v},t) = \delta f_0[\vec{x}\,'(0;\vec{x},\vec{v},t),\vec{v}\,'(0;\vec{x},\vec{v},t)] - \int_0^t dt' \left.\frac{\delta\vec{F}}{m}\cdot\frac{\partial f_0}{\partial\vec{v}}\right|_{(\vec{x}\,',\vec{v}\,',t')},$$

where $\delta f_0(\vec{x},\vec{v}) = \delta f(\vec{x},\vec{v},t=0)$ is the initial distribution perturbation, and the unperturbed trajectory now verifies

$$\begin{aligned}
\frac{d\vec{x}\,'(t')}{dt'} &= \vec{v}\,'(t'), \\
\frac{d\vec{v}\,'(t')}{dt'} &= \frac{q}{m}\vec{F}_0[\vec{x}\,'(t'),\vec{v}\,'(t'),t'].
\end{aligned}$$

with initial conditions

$$\vec{x}\,'(t'=t) = \vec{x}, \qquad \text{and} \qquad \vec{v}\,'(t'=t) = \vec{v}.$$

Bibliography

[1] R. Z. Sagdeev and A. A. Galeev, *Nonlinear Plasma Theory* (W. A. Benjamin, Inc., New York, 1969).

[2] K. Appert, *Théorie des Plasmas Chauds* (EPFL-Repro, EPFL, 2003).

[3] J. R. Danielson, F. Anderegg, and C. F. Driscoll, Physical Review Letters **92**, #245003 (2004).

[4] L. D. Landau and E. M. Lifshitz, *Electrodynamics of Continuous Media, Vol. 8 of Course of Theoretical Physics* (Pergamon Press, Oxford, 1960).

[5] M.Abramowitz and I.A.Stegun, *Handbook of Mathematical Functions with Formulas, Graphs, and Mathematical Tables* (John Wiley & Sons, New York, 1964).

[6] T. O'Neil, Physics of Fluids **8**, 2255 (1965).

[7] I. B. Bernstein, J. M. Greene, and M. D. Kruskal, Physical Review **108**, 546 (1957).

[8] G. J. Morales and T. O'Neil, Physical Review Letters **28**, 417 (1972).

[9] R. L. Dewar, Physics of Fluids **15**, 712 (1972).

[10] W. L. Kruer, J. M. Dawson, and R. N. Sudan, Physical Review Letters **23**, 838 (1969).

[11] M. Goldman, Physics of Fluids **13**, 1281 (1970).

[12] R. L. Dewar, W. L. Kruer, and W. M. Manheimer, Physical Review Letters **28**, 215 (1972).

[13] W. L. Kruer, *The Physics of Laser Plasma Interactions, Frontiers in Physics* (Addison-Wesley Publishing Co., Redwood City, California, 1988).

[14] M. N. Rosenbluth, Physical Review Letters **29**, 565 (1972).

[15] J. F. Drake *et al.*, Physics of Fluids **17**, 778 (1974).

[16] H. X. Vu, D. F. DuBois, and B. Bezzerides, Physical Review Letters **86**, 4306 (2001).

[17] S. Brunner and E. J. Valeo, Physical Review Letters **93**, 145003 (2004).

[18] G. Shvets, N. J. Fisch, A. Pukhov, and J. M. ter Vehn, Physical Review Letters **81**, 4879 (1998).

[19] V. M. Malkin, G. Shvets, and N. J. Fisch, Physical Review Letters **82**, 4448 (1999).

[20] D. S. Clark, Ph.D. thesis, Princeton University, 2003.

[21] Y. Ping *et al.*, Physical Review Letters **92**, #175007 (2004).